express
polymer letters

Research article

Metalloalkoxysiloxanes-cured polydimethylsiloxane compositions filled with silica component for special applications: Dielectric and mechanical properties

Alexander N. Tarasenkov[1*] *, Maria S. Parshina*[1,2] *, Nadezhda A. Tebeneva*[1] *,*
Kirill M. Borisov[1] *, Galina P. Goncharuk*[1] *, Vitaliy G. Shevchenko*[1] *,*
Sergey A. Ponomarenko[1] *, Aziz M. Muzafarov*[1,2]

[1]Institute of Synthetic Polymeric Materials, Russian Academy of Sciences, Profsoyuznaya St. 70. 117393, Moscow, Russia
[2]Nesmeyanov Institute of Organoelement Compounds, Russian Academy of Sciences, V-334, Vavilova St. 28, 119991 Moscow, Russia

Abstract. The dielectric and mechanical properties of a wide range of polydimethylsiloxane-based compositions filled with silica component and cured with various metallosiloxanes have been studied. It is shown that the resulting systems are typical dielectrics. Silica component introduction in combination with the metal-siloxane network formation in the material can significantly increase its dielectric permittivity and conductivity in the frequency range $<10^2$ Hz compared to commercial silicon compounds and pure PDMS. It is found that varying the metallosiloxane structure and composition and the degree of silica filling are effective tools for changing the dielectric parameters of the material - up to ~5–10 at 1–10 Hz. By varying the functionality and length of the rubber chain, as well as the curing rate, it is possible to vary the mechanical properties of the material within a wide range – 2–10 MPa strength and elongation up to 500% with the pure elastomeric properties up to 200%. This approach to the formation of material opens up prospects for using such cured systems as dielectric elastomers for special applications such as flexible capacitive sensors or actuators for medical and robotic applications.

Keywords: polymer composites, nanocomposites, material testing, metalloalkoxysiloxanes, silicon

1. Introduction

Dielectric elastomers are currently being used in motors, optical devices, sensors, energy storage, robotics, etc., including artificial muscles applications [1]. Implementation of the latter requires the creation of a so-called 'actuator', the main functional element of which is an electroactive polymer (EAP) capable of being polarized and, as a consequence, changing its size and shape under the applied electric field [2–4]. EAPs, or so-called dielectric elastomers, can be performed as electrochemical polymers using electrically driven mass transport of ions or electrically charged species to effect a charge in the shape and field-activated polymers using an electric field to effect a shape change by acting directly on charges within the polymer (or vice versa) [5].

The active study of the filled cross-linked systems behavior under various external conditions began in the 80s of the 20th century, and in the 90s, the main approaches were already formulated, in particular, the implementation of the concept of artificial muscles creating using dielectric elastomers [6, 7]. Despite

---

the many approaches developed, there is currently a surge of interest in creating new approaches for so-called 'soft actuators' creating based on EAPs.

Depending on the potential application area, EAP should have a number of required characteristics [8], the most important of which are the increased dielectric constant, mechanical strength (0.1–25 MPa), and the ability to develop large reversible deformations (not less than 100%), while maintaining conductivity. Among the polymers that can be used, are, for example, fluoropolymers, polyacrylates, polyurethanes, and silicones [2, 9–12]. Among the advantages of these classes of polymers (for example, high piezoelectric response due to the presence of polar groups), silicone elastomers have a number of features defined their use as dielectric elastomers in actuators such as a wide range of mechanical properties regulation, a long exploitation period, a wide range of operating temperatures, biostability, the possibility of in situ cross-linking and molding, in particular by 3D printing [13], as well as high response speed and energy density when voltage is applied to the electrodes [14], relatively low dielectric and mechanical losses [5]. However, silicones have a relatively low dielectric constant [15], which necessitates the use of high voltage to activate the energy converter. The main approaches to increasing the dielectric permittivity of silicones are the use of fillers and chemical modification.

Filling involves the introduction of conductive or high-dielectric fillers at the mixing stage. Such fillers can be complex inorganic salts [16, 17], carbon nanofillers of various morphology and composition [18–21], as well as metal oxides in nano- or micro-sized form [22–25]. Filling allows increases not only the dielectric constant and conductivity but also strengthens the material. In particular, using graphene particles or carbon nanotubes (one of the sizes no more than 100 nm) makes it possible to silicone rubber reinforce using smaller amounts of filler compared to technical carbon, which has little effect on the viscoelastic properties of the material [26, 27]. One of the most common approaches is the introduction of nano- and micro-sized silica into silicone material: it not only has a good affinity for silicone but also increases and stabilizes the dielectric characteristics and strengthens the material [28, 29]. However, this approach has a problem with filler distribution over the material volume. Consequently, the filler should be compatible with the polymer matrix, have a low

aggregation degree, and uniformly fill the material pores [30].

Chemical modification of silicon consists of introducing groups with a high dipole moment directly into the polymer matrix structure or initial monomer [31–33]. Click chemistry, in particular, hydrothiolation opens up wide possibilities for fast modification of vinyl-containing silicone chains [34, 35]. Among the methods, one can also note the production of elastomeric interpenetrating networks [36]. Each method has its limitations, primarily related to changes in the physicochemical properties of the matrix during modification and compatibility of mixture components.

We have previously demonstrated the approach of cross-linked silicone material formation by using functional metallosiloxanes [37]. In this case, we not only introduce a metal oxide component into the material but also introduce a silica component and ensure the uniform distribution of all the components in the final material since it forms from completely liquid precursors. This paper deals with the dielectric and mechanical properties of silica-filled cross-linked compositions obtained in this way. We believe the use of functional metallosiloxanes as silicone compositions hardeners is a promising approach to obtaining electroactive silicon materials.

2. Experimental

Elemental analysis was carried out on a 'Carlo Erba 1106' instrument (Italy). The relative error of determination of the contents of silicon, carbon, and hydrogen did not exceed 0.1 wt%. The silicon, carbon, and hydrogen contents were determined by burning a sample ($5 \cdot 10 \cdot 10^{-3}$ g) in an oxygen gas atmosphere at 950 °C.

The real and imaginary parts of permittivity, conductivity, modulus, and the loss factor were measured using an impedance analyzer 'Novocontrol Alpha-A' (Installation Concept 40) and the dielectric cell 'ZGS Alpha Active Sample Cell' with gold disk electrodes with the diameter of 20 mm. Measurements were performed in the frequency range of 10^{-1}–10^6 Hz.

Scanning electron microscopy (SEM) was performed using a JCM-6000 PLUS microscope equipped with an energy-dispersive spectrometer at accelerating voltages of 5–15 kV.

The mechanical properties of the compositions were determined in the uniaxial extension mode on the universal testing machine Autograph AGS-H by

Shimadzu (Japan). The samples were strips with a working part size of 3×20 mm; the rate of the extension was 10 mm/min. The tensile strength (σ) and elongation (ε) at break were measured.

To prepare the compositions, commercially available polydimethylsiloxane (PDMS) rubbers under the trademarks 'СКТН-Г' and 'СКТН-Е' (further PDMS-G and PDMS-E respectively) of different molecular weight were used. The products are characterized by small molecular weight and dynamic viscosity values: PDMS-G – M_w ~ 55 000 g/mol, 5–9 Pa·s, and PDMS-E – M_w ~ 120 000 g/mol, 80–120 Pa·s. Anhydrous metal chlorides were used without further purification: $AlCl_3$ (≥99%, 'Fluka Analytical'), $FeCl_3$ (≥98.5%, 'Carl Roth'), $ZrCl4$ (≥99.5%, 'Lanhit'), $ZnCl_2$ (≥99.9%, 'Lanhit'), $CuCl_2$ (≥99.9%, 'Lanhit'), WCl_6 (≥99.9%, 'Lanhit'). Methyltriethoxysilane, phenyltriethoxysilane, and vinyltriethoxysilane were distilled under argon before use. Toluene and ethanol were dried by prolonged boiling, followed by distillation over CaH_2 under argon, and stored over 3 Å molecular sieves. Hyperbranched polyethoxysiloxane (PEOS) was prepared according to the procedure [38].

Non-fully (alkyldiethoxy)siloxy substituted metal-losiloxanes $[OEt]_xM[OSi(R)(OEt)_2]_k$ were obtained according to the method [37].

Synthesis of diethoxy-bis-(methyldiethoxysiloxy) zirconium Zr-Me(2-2) and diethoxy-bis-(phenyl-diethoxysiloxy)zirconium Zr-Ph(2-2) presented in work [37].

Triethoxy(phenyldiethoxysiloxy)zirconium Zr-Ph(1-3) was obtained similarly to Zr-Ph(2-2) by interaction of zirconium (IV) chloride (11.03 g, 0.0473 mol) suspension in 100 ml of dried toluene with a mixture of sodium metal solution (3.26 g, 0.1419 mol) in 65 ml of dried ethanol (9.66 g, 0.1419 mol of sodium ethylate) and a solution of sodium phenyldiethoxysi-lanolate (11.08 g, 0.0473 mol) in 150 ml of dried toluene. The reaction mixture was stirred for 3 hrs at 50 °C. After separation from the precipitate, 100 ml of dried toluene was added to the mother liquor, and ~200 ml of solvent was then distilled to get rid of ethanol. A transparent colorless solution was obtained. The dry product was a colorless transparent non-flowing substance. The yield of the product was 20.30 g (98%). Found [%]: C, 43.74; H, 6.80; Si, 6.35; Zr, 21.06. $C_{16}H_{30}O_6SiZr$. Calculated [%]: C, 43.90; H, 6.91; Si, 6.42; Zr, 20.84.

In the case of sodium vinyldiethoxysilanolate $NaOSi(Vin)(OEt)_2$, all operations were carried out in an argon atmosphere. Sodium hydroxide (2.40 g, 0.060 mol) was added to a solution of vinyltri-ethoxysilane (11.42 g, 0.060 mol) in 30 ml of dried toluene at stirring. The mixture was stirred at room temperature until sodium hydroxide was completely dissolved (~30 min). The resulting mixture was evaporated from volatiles in a vacuum (1 Torr) at 50 °C. 10.66 g (97%) of the white pasty mass was obtained. Diethoxy-bis-(vinyldiethoxysiloxy)zirconium Zr-Vin(2-2) was obtained similarly to Zr-Ph(2-2) by the interaction of zirconium (IV) chloride (3.37 g, 0.0145 mol) suspension in 20 ml of dried toluene with a mixture of sodium metal solution (0.667 g, 0.0290 mol) in 14 ml of dried ethanol (1.97 g, 0.0290 mol of sodium ethylate) and solution of sodium vinyldiethoxysilanolate (5.23 g, 0.0284 mol) in 30 ml of dried toluene. The reaction mixture was stirred for 2 hrs at 50 °C. After separation from the precipitate, 70 ml of dried toluene was added to the mother liquor, and ~100 ml of solvent was distilled to get rid of ethanol. A clear orange solution was obtained. The dry product was an orange transparent, highly viscous liquid. The yield of the product was 6.32 g (86%). Found [%]: C, 34.29; H, 6.30; Si, 11.22; Zr, 19.65. $C_{16}H_{36}O_8Si_2Zr$. Calculated [%]: C, 38.14; H, 7.20; Si, 11.15; Zr, 18.11.

Triethoxy-tris-(phenyldiethoxysiloxy)tungsten W-Ph(3-3) was obtained similarly to Zr-Ph(2-2) by the interaction of tungsten (VI) chloride (3.79 g, 0.0096 mol) suspension in 30 ml of dried toluene, first with a solution of sodium phenyldiethoxysilanolate (6.70 g, 0.0286 mol) in 50 ml of dried toluene, then with a mixture of a solution of metallic sodium (0.66 g, 0.0286 mol) in 13 ml of dried ethanol (1.96 g, 0.0286 mol of sodium ethylate) and 40 ml of dried monoglim. The mixture was stirred for 5 hrs at 50 °C. After separation from the precipitate, a clear dark orange solution was obtained. The dry product was a dark orange heterogeneous substance. The yield of the product was 7.25 g (79%). Found [%]: C, 45.27; H, 6.18; Si, 8.57; W, 19.14. $C_{36}H_{60}O_{12}Si_3W$. Calculated [%]: C, 45.37; H, 6.35; Si, 8.84; W, 19.29.

Tetrakis-(vinyldiethoxysiloxy)zirconium Zr-Vin(4-0) was obtained according to the method [30] by the interaction of zirconium (IV) chloride (3.49 g, 0.0150 mol) suspension in 50 ml of dried toluene with a solution of sodium vinyldiethoxysilanolate

(10.66 g, 0.0578 mol) in 100 ml of dried toluene. The reaction mixture was stirred for 4 hrs at 50 °C. After separation from the precipitate, a transparent, colorless solution was obtained. The dry product was a colorless transparent viscous liquid. The yield of the product was 6.26 g (57%). Found [%]: C, 33.90; H, 5.74; Si, 17.06; Zr, 10.88. $C_{24}H_{52}O_{12}Si_4Zr$. Calculated [%]: C, 39.15; H, 7.12; Si, 15.26; Zr, 12.39.

Fully (phenyldiethoxy)siloxy-substituted metallosiloxanes $M[OSi(Ph)(OEt)2]x$ were obtained according to the method [39].

Synthesis of tris-(phenyldiethoxysiloxy)iron Fe-Ph(3-0) presented in work [40].

Tris-(phenyldiethoxysiloxy)aluminum Al-Ph(3-0) was obtained by the interaction of aluminum (III) chloride (5.37 g, 0.0403 mol) suspension in 50 ml of dried toluene with a sodium phenyldiethoxysilanolate (28.30 g, 0.1208 mol) solution in 180 ml of dried toluene. The reaction mixture was stirred for 3 hrs at 50 °C. After separation from the precipitate, a transparent, colorless solution was obtained. The dry product was a colorless transparent viscous liquid. The yield of the product was 22.52 g (85%). Found [%]: C, 54.54; H, 6.78; Si, 12.81; Al 4.11. $C_{30}H_{45}O_9Si_3Al$. Calculated [%]: C, 54.52; H, 6.86; Si, 12.75; Al, 4.08.

Bis-(phenyldiethoxysiloxy)copper Cu-Ph(2-0) was obtained by interaction of copper (II) chloride (1.27 g, 0.0095 mol) solution in 5 ml of dried ethanol with a sodium phenyldiethoxysilanolate (4.48 g, 0.019 mol) solution in 30 ml of dried toluene. The reaction mixture was stirred for 1 hr at 60 °C. After separation from the precipitate, a turquoise solution was obtained. The dry product was a dark turquoise transparent viscous liquid. The yield of the product was 2.76 g (60%). Found [%]: C, 51.11; H, 4.84; Si, 16.63; Cu. $C_{20}H_{30}O_6Si_2Cu$. Calculated [%]: C, 49.41; H, 6.22; Si, 11.55; Cu, 13.07.

Bis-(phenyldiethoxysiloxy)zinc Zn-Ph(2-0) was obtained by interaction of zinc (II) chloride (5.56 g, 0.0408 mol) solution in 25 ml of dried ethanol with a sodium phenyldiethoxysilanolate (19.12 g,

0.0816 mol) solution in 150 ml of dried toluene. The reaction mixture was stirred for 3 hrs at 60 °C. After separation from the precipitate, a colorless transparent solution was obtained. The dry product was a solid colorless substance. The yield of the product was 13.35 g (67 %). Found [%]: C, 49.40; H, 6.32; Si, 11.52; Zn, 13.28. $C_{20}H_{30}O_6Si_2Zn$. Calculated [%]: C, 49.22; H, 6.20; Si, 11.51; Zn, 13.40.

2.1. Preparation of compositions

Toluene solution of initial components (polydimethylsiloxane rubber, hyperbranched polyethoxysiloxane, and metallosiloxane) was poured onto a Teflon® substrate and then kept at room temperature until most volatiles were evaporated. After that residual was heated following the temperature steps: 1 hour at 50 °C, then 1 hour at 70 °C, then 1 hour at 100 °C, and finally 2 hours at 150 °C. The compositions were cooled, removed from the substrate, and then tested.

3. Results

Metalloorganoalkoxysiloxanes (after this MS) are compounds containing M–O–Si bonds in their structure (M – metal atom), where the silicon atom is functionalized by alkoxy groups and can also be associated with any organic group (Figure 1). Previously, we presented data on the synthesis of such compounds from various metal chlorides and Rebrov salts, as well as sodium alcoholates [37, 39]. The key point of synthesis is the ability to vary not only the type of metal atom and organic group but also the number of alkoxy groups in the MS structure (Figure 1).

The use of alcoholates along with Rebrov salts makes it possible to obtain mixed-type MSs in which the metal atom is only partially shielded by the siloxy fragment and directly connected to the alkoxy group. Such compounds have increased activity relative to the hydrolysis and condensation processes of alkoxysilanes. The condensation process of alkoxysilyl groups of MS, in turn, is activated by the catalytic
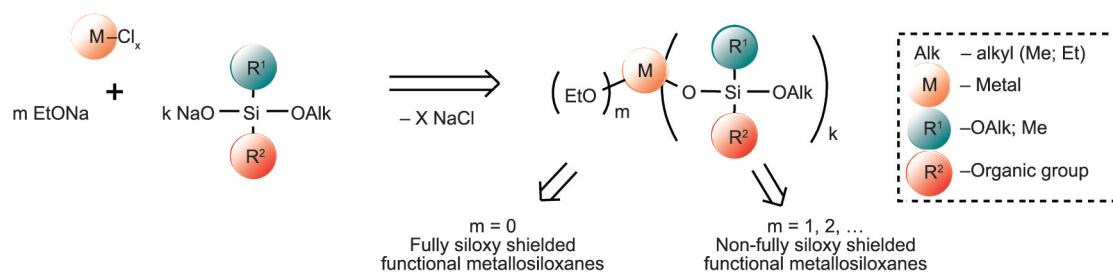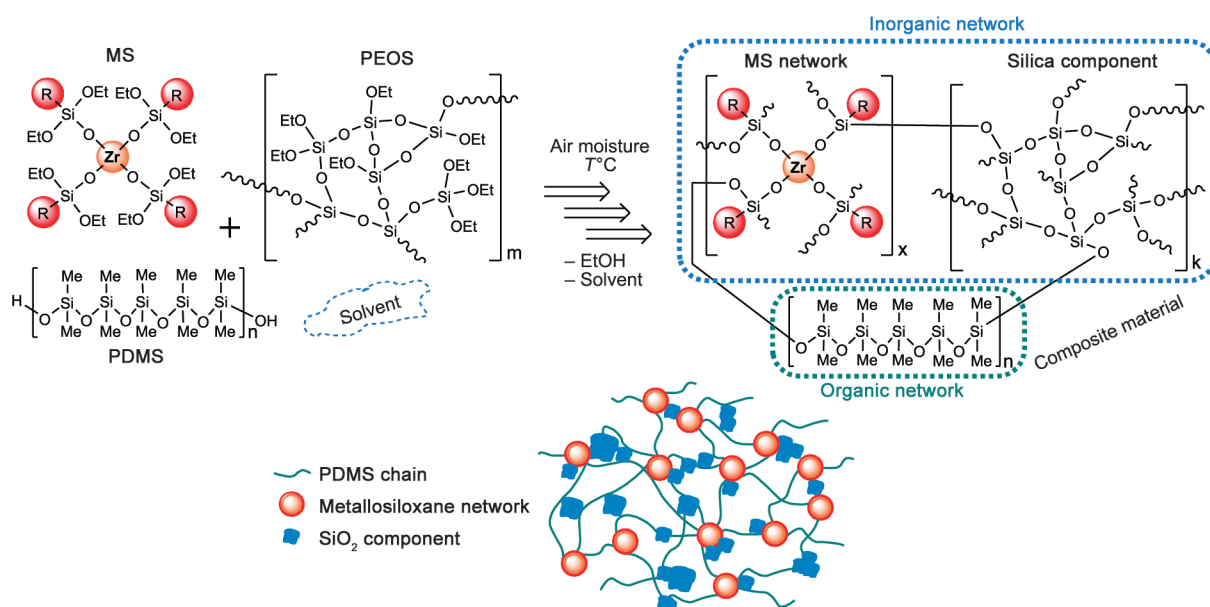

Figure 1. General scheme of metalloorganoalkoxysiloxanes synthesis.

Figure 2. Chemistry of the formation process of three-component composite material based on polydimethylsiloxane on the example of zirconium siloxane.

properties of the metal. *I.e.*, we have a highly effective vulcanizing agent for silicone rubbers, capable of both embedding into the forming organic silicone network and forming its inorganic metal-silica network during the material formation (Figure 2). At the same time, we avoid metal aggregation processes since each metal atom is isolated by a siloxy substituent and is evenly distributed over the final composite volume [37].

This method of material production seems to us promising for the creation of new elastomeric materials with adjustable dielectric and mechanical properties due to the possibility of varying the ratio of the initial components, a metal atom type, and an organic substituent at silicon atom.

Table 1 shows data on dielectric constant (ε') and conductivity (σ') at various frequencies (f = 0.1, 1, 10, 100 Hz) for some of the compositions described above. It can be seen that for two-component compositions without a silica component; the dielectric constant values are in the range of 2.5–3.0 over the entire frequency range, which approximately corresponds to the values for industrial silicones and pure polydimethylsiloxane [15]. A slight increase in the dielectric constant occurs for three-component systems filled with silica component. The same goes for

Table 1. Values of dielectric constant and conductivity for some of the compositions.

#	Initial components of the composition		Weight ratio [–]	ε' [–]	σ' [$\cdot 10^{11}$ S/cm]
					f = 0.1/1/10/100 Hz
1	Fe[OSi**Me**(OEt)$_2$]$_3$	PDMS-A[a]	–	2/3	2.7/2.7/2.6/2.6	0.0002/0.001/0.005/0.04
2	[OEt]$_2$Fe[OSi**Me**(OEt)$_2$]$_1$	PDMS-A	–	2/3	3.6/3.4/3.4/3.4	0.002/0.004/0.015/0.08
3	Fe[OSi**Me**(OEt)$_2$]$_3$	PDMS-D[b]	–	2/3	2.6/2.5/2.5/2.5	0.0001/0.0006/0.003/0.03
4	Fe[OSi**Me**(OEt)$_2$]$_3$	PDMS-D	–	3/3	2.9/2.8/2.8/2.8	0.0002/0.001/0.005/0.04
5	Fe[OSi**Me**(OEt)$_2$]$_3$	PDMS-A	PEOS	2/3/1	3.0/2.8/2.8/2.8	0.002/0.005/0.02/0.08
6	Fe[OSi**Me**(OEt)$_2$]$_3$	PDMS-D	PEOS	2/3/1	5.0/3.7/3.3/3.1	0.01/0.04/0.11/0.37
7	Zr[OSi**Me**(OEt)$_2$]$_4$	PDMS-E[c]	–	1/3	2.6/2.5/2.5/2.5	0.0005/0.002/0.01/0.04
8	Zr[OSi**Me**(OEt)$_2$]$_4$	PDMS-D	PEOS	1/3/1	3.6/2.6/2.3/2.2	0.008/0.03/0.09/0.28
9	Zr[OSi**Ph**(OEt)$_2$]$_4$	PDMS-D	PEOS	1/3/1	13.3/6.0/4.0/3.2	0.13/0.27/0.67/2.23
10	Al[OSi**Me**(OEt)$_2$]$_3$	PDMS-E	–	1/3	2.5/2.4/2.4/2.4	0.0003/0.001/0.003/0.02
11	Nb[OSi**Me**(OEt)$_2$]$_5$	PDMS-D	PEOS	1/3/1	3.6/2.6/2.3/2.2	0.008/0.03/0.09/0.28

[a]Polydimethylsiloxane rubber with M_w ~ 20 000 g/mol pre-blocked with 3-aminopropyltriethoxysilane;
[b]Silanol-terminated polydimethylsiloxane rubber with M_w ~ 90 000 g/mol;
[c]silanol-terminated polydimethylsiloxane rubber with M_w ~ 120 000 g/mol.

conductivity. *I.e.*, it can be argued that the dielectric properties of such systems can be regulated.

An important factor is the mechanical characteristics of the final material. In previous studies, we have shown that Zr-siloxanes are the most optimal with respect to the cross-linking activity and mechanical properties of the resulting films. Therefore, the present study mostly concerns the materials obtained with the use of Zr-siloxanes.

3.1. Investigation of compositions with Zr-siloxane

Fully and partially substituted alkyldiethoxysiloxy derivatives of Zr-siloxanes were used in the work, differing both in the degree of shielding of the metal atom by a silicon substituent and by an organic substituent at the silicon atom. The structure and designations of the used compounds are shown in Figure 3. Mainly, partially siloxy substituted MSs were used due to their greater activity, as well as the ability to form Zr–O–Zr bonds during hydrolysis and condensation, which may affect the properties of the material. Methylsilyl derivative Zr-Me(2-2) (diethoxy-bis-(methyldiethoxysiloxy)zirconium) was used in a variant containing, on average, two siloxy and two ethoxy substituents per molecule. The effect of the metallosiloxane composition on the mechanical and dielectric properties of materials was studied in the example of phenylsilyl derivatives therefore, they were obtained and used in three variants: fully- Zr-Ph(4-0) and partially siloxy substituted, containing two Zr-Ph(2-2) or one Zr-Ph(1-3) siloxy substituent (tetrakis-, diethoxy-bis- and triethoxy-(phenyldiethoxysiloxy)zirconium, respectively). Vinyl derivatives were obtained in two variants: fully siloxy substituted – tetrakis-(vinyldiethoxysiloxy)zirconium Zr-Vin(4-0), and as an analog of methyl and phenyl derivatives – diethoxy-bis-(vinyldiethoxysiloxy)zirconium Zr-Vin(2-2). Metallosiloxanes were synthesized according to Figure 1 in toluene and
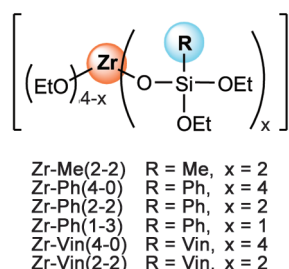
ethanol (in the case of ethoxy-zirconium derivatives). Metallosiloxanes were stored and used in the form of dilute toluene solutions (~20% by weight) under an inertia layer without air access due to the high reactivity in the presence of air moisture. Chromatographic analysis of such compounds is not possible, and their identification was carried out using elemental analysis. The elemental composition of all the obtained products is in good agreement with the calculated content of the elements.

To study the dielectric properties, a number of two- and three-component cured silicone compositions based on polydimethylsiloxane (PDMS) were obtained. The third component was branched polyethoxysiloxane (PEOS), a silica precursor, which can potentially form nanoscale silica inside the material after curing (the so-called 'liquid filling'), being part of an inorganic network along with a metallosiloxane three-dimensional network (Figure 2).

The compositions were obtained in the form of films 0.35±0.03 mm thick. Low molecular weight rubber of the trademark 'CKTH-E' (after this PDMS-E) was mainly used as PDMS, having sufficient molecular weight (M_w ~ 120 000 g/mol) to produce elastomers, but at the same time fluid and having good solubility in organic solvents. The weight of the rubber was taken as a basis for the calculation, and the number of MS and PEOS varied relative to it. A similar calculation scheme was carried out by us in previous works [28, 30]. The initial ratio of PEOS/MS in the mixture generally varied from 0/2 to 4/1pending on the activity of MS and the quality of the compositions obtained. *I.e.*, it was studied the systems obtained in the maximum possible range of metallosiloxane and silica components filling with the preservation of homogeneity and the absence of obvious brittleness. Thus, in all cases, the compositions were characterized by an excess of ethoxysilyl groups of metallosiloxane and liquid filler relative to the hydroxyl groups of PDMS at the initial stage, which determined the course of two parallel processes during the material formation: rubber vulcanization (organic network formation) and the formation of a three-dimensional network of metallosiloxane and silica (inorganic network formation). For comparison, we investigated the dielectric properties of a film obtained from commercially available two-component cured silicone of the Ecoflex® brand. Tables 2–4 below provide data on the dielectric and mechanical properties of the compositions.

Zr-Me(2-2)	R = Me, x = 2
Zr-Ph(4-0)	R = Ph, x = 4
Zr-Ph(2-2)	R = Ph, x = 2
Zr-Ph(1-3)	R = Ph, x = 1
Zr-Vin(4-0)	R = Vin, x = 4
Zr-Vin(2-2)	R = Vin, x = 2

Figure 3. Zr-siloxanes used in the work.

Table 2 presents data for compositions cured with methylsilyl derivatives of Zr-siloxane Zr-Me(2-2). This metallosiloxane has a high vulcanization activity relative to both pure PDMS and in a mixture with PEOS. However, it can be seen that with an increase in the metallosiloxane component content, the compositions are brittle and not subject to further investigation due to the lack of elastomeric properties. Films of acceptable quality can be obtained only with an increase in the PEOS/MS ratio, *i.e.*, at high silica component filling. Nevertheless, in all cases, homogeneous transparent compositions are obtained, *i.e.*, there is full compatibility of the final components of the system. In the aspect of electrical properties, there is a tendency to increase in the dielectric constant in the low-frequency region $f < 10$ Hz with an increase in the initial PEOS/MS ratio. And if the two-component system (Table 2 #1) is close in terms of pure PDMS ($\varepsilon' \sim 2.5$), then with an increase in silica component filling, this dielectric constant values increase to $\varepsilon' \sim 3.6–4.1$ respectively (Table 2 #7).

Table 3 presents data for compositions cured with phenylsilyl derivatives of Zr-siloxanes. Unlike methylsilyl derivatives, in this case it is possible to obtain films of acceptable quality practically over the entire range of the initial ratios PEOS/MS, even with a high initial MS content. As in the previous case, the dielectric constant (ε') of a system that does not contain silica component (Table 3 #13 and Table 4 #2, 3) are approximated, in particular, to those for Ecoflex® films ($\varepsilon' \sim 3.6–2.9$ and $\varepsilon'' \sim 0.9–0.03$). In the case of systems filled with silica, the values of ε' and ε'' are noticeably higher than the standard ones, especially their sharp increase is observed in the low-frequency range $f < 10$ Hz, and the higher the initial PEOS/MS ratio, the greater the observed standard deviation (Figure 4). Using phenylsilyl Zr-siloxanes derivatives allowed us to evaluate the effect of MS composition on the quality and dielectric parameters of the compositions obtained. In the Zr-Ph(4-0) → Zr-Ph(2-2) → Zr-Ph(1-3) row decreases the number of phenyl and ethoxy groups of hardener but at the same time increases its activity relative to the condensation reaction of all initial components of the mixture. When using Zr-Ph(1-3), compositions appear more homogeneous, but at the same time, they become more fragile with increasing MS and silica component filling. And in the case of Zr-Ph(4-0), a more elastic material was obtained; however, the final film tends to opalescence with an

Table 2. Mechanical and dielectric characteristics at different frequencies for the compositions obtained using Zr-Me(2-2).

#	Initial weight ratio MS/PDMS-E/PEOS	ε' [–]	ε'' [–]	σ' [·10^{11} S/cm]	$\tan\delta$ [–]	$\sigma \pm \Delta\sigma$ $\varepsilon \pm \Delta\varepsilon$ [MPa/%]	Characterization
			$f = 0.1/1/10/100$ Hz				
1	1/3/0	2.7/2.6/2.6/2.6	0.05/0.02/0.01/0.01	0.0003/0.001/0.01/0.04	0.02/0.009/0.004/0.003	2.1±0.1 347±30	Homogeneous, transparent, colorless
2	2/3/0	–	–	–	–	–	Homogeneous, transparent, colorless, cracking by volume
3	2/3/1	–	–	–	–	–	
4	1/3/1	3.3/3.2/3.1/3.1	0.2/0.1/0.03/0.01	0.001/0.005/0.02/0.09	0.07/0.03/0.01/0.005	4.8±0.1 63±6	Homogeneous, transparent, colorless
5	2/3/2	–	–	–	–	–	Homogeneous, transparent, yellowish, cracking by volume
6	1/3/2	4.2/3.6/3.5/3.4	0.8/0.27/0.08/0.02	0.005/0.02/0.05/0.14	0.19/0.07/0.02/0.01	4.0±0.4 4±1	Homogeneous, transparent, yellowish
7	1/3/3	5.6/4.1/3.6/3.7	3.0/0.7/0.2/0.06	0.02/0.04/0.12/0.31	0.53/0.18/0.05/0.02	5.0±0.5 3±1	

(Zr-Me(2-2))

Table 3. Mechanical and dielectric characteristics at different frequencies for the compositions obtained using Zr-Ph-siloxanes.

| #		Initial weight ratio MS/PDMS-E/PEOS	ε' [-]	ε'' [-]	σ' [·10^{11} S/cm]	tanδ [-]	$\frac{\sigma \pm \Delta\sigma}{\epsilon \pm \Delta\epsilon}$ [MPa/%]	Characterization
					f = 0.1/1/10/100 Hz			
1		3/3(E)/1	8.3/4.9/3.8/3.6	7.5/1.8/0.5/0.1	0.04/0.10/0.28/0.76	0.90/0.37/0.12/0.04	6.3±0.5 / 723±59 b	Homogeneous, slightly opalescent, yellowish
2		2/3(E)/1	5.9/4.0/3.3/3.2	4.3/1.1/0.3/0.1	0.02/0.06/0.16/0.44	0.74/0.27/0.08/0.02	5.1±0.5 / 635±38 b	
3		1/3(E)/1	8.5/4.9/3.5/3.2	8.8/2.0/0.6/0.2	0.05/0.12/0.36/0.92	1.04/0.04/0.17/0.05	3.9±0.2 / 566±36	Homogeneous, transparent, yellowish
4	Zr-Ph(4-0)	2/3(E)/2	11.2/5.4/4.0/3.7	15.7/3.0/0.7/0.2	0.09/0.17/0.40/0.85	1.40/0.55/0.17/0.05	5.9±0.6 / 417±123 b	
5		1/3(E)/2	10.3/7.1/4.5/3.8	2.9/2.0/1.2/0.3	0.02/0.11/0.69/1.68	0.28/0.28/0.25/0.08	5.6±0.3 (3.7±0.4)c / 14±2 (465±43)	
6		1/3(E*)/2	8.6/5.1/3.8/3.4	6.5/2.0/0.6/0.2	0.04/0.11/0.33/0.87	0.76/0.38/0.15/0.05	5.2±0.5 / 347±32	
7		1/3(G)/2	10.8/5.8/4.1/3.7	10.6/2.7/0.8/0.2	0.06/0.15/0.46/1.07	0.98/0.46/0.19/0.05	6.4±0.3 / 341±33	
8		1/3(E)/3	34.5/8.7/5.4/4.4	71.7/11.7/2.1/0.6	0.40/0.66/1.26/3.20	2.08/1.34/0.39/0.13	5.5±0.3 / 96±30 b	
9		1/3(G)/3	13.5/7.5/4.6/3.8	12.0/3.5/1.3/0.3	0.067/0.20/0.77/1.75	0.89/0.47/0.28/0.08	6.1±0.2 / 257±16	
10		0.5/3(E)/2	22.1/7.2/4.4/3.8	27.7/6.5/1.3/0.3	0.02/0.37/0.79/1.94	1.25/0.90/0.30/0.09	5.6±0.1 / 16±2	
11		1/3(E)/5	19.8/8.7/4.9/4.1	39.8/7.2/1.8/0.4	0.22/0.41/1.08/2.20	2.01/0.83/0.37/0.10	4.1±0.1 / 121±59 b	
12		1/3(G)/5	22.8/7.6/5.0/4.3	33.1/6.8/1.3/0.4	0.18/0.39/0.80/2.04	1.45/0.89/0.27/0.08	8.5±0.1 / 21±1 b	

Table 3. Continuation 1.

#	Initial weight ratio MS/PDMS-E/PEOS	ε' [–]	ε'' [–]	σ' [·10^{11} S/cm]	$\tan\delta$ [–]	$\dfrac{\sigma \pm \Delta\sigma}{\varepsilon \pm \Delta\varepsilon}$ [MPa/%]	Characterization
				$f = 0.1/1/10/100$ Hz			
13	2/3(E)/0	3.6/3.1/2.9/2.9	0.9/0.25/0.1/0.03	0.005/0.01/0.04/0.16	0.26/0.08/0.03/0.01	3.9±0.4 / 618±29	Homogeneous, transparent, yellowish
14	3/3(E)/1	7.7/4.7/3.9/3.6	7.3/1.6/0.4/0.1	0.04/0.09/0.24/0.73	0.95/0.34/0.10/0.04	5.2±0.2 / 258±115[b]	
15	2/3(E)/1	5.9/4.0/3.5/3.3	3.9/0.9/0.3/0.1	0.02/0.05/0.15/0.47	0.66/0.24/0.07/0.02	5.3±0.2 / 595±63[b]	
16	1/3(E)/1	7.5/4.6/3.6/3.3	6.8/1.7/0.5/0.1	0.04/0.09/0.29/0.85	0.90/0.36/0.14/0.05	4.7±0.3 / 322±30	
17	2/3(E)/2	12.8/5.6/4.0/3.6	13.3/3.1/0.7/0.2	0.074/0.18/0.44/1.19	1.05/0.56/0.18/0.06	8.3±0.2 / 14±1	
18	1/3(E)/2	14.4/5.8/4.1/3.6	18.2/3.7/0.8/0.2	0.10/0.21/0.50/1.31	1.27/0.64/0.21/0.07	6.5±0.1 / 35±3	
19	1/3 (G)/2	13.6/6.0/4.3/3.8	22.4/4.0/0.9/0.3	0.12/0.23/0.54/1.39	1.65/0.66/0.21/0.07	7.9±0.2 / 145±15	
20	1/3(E)/3	12.4/6.3/3.8/3.2	7.3/3.3/1.0/0.3	0.041/0.19/0.61/1.82	0.59/0.52/0.27/0.10	7.9±0.3 / 13±1	
21	1/3(G)/3	18.5/6.4/4.4/3.9	27.1/5.1/1.1/0.3	0.15/0.29/0.63/1.54	1.47/0.80/0.24/0.06	10.6±0.8 / 24±2	
22	0.5/3(E)/2	7.3/6.5/4.7/3.8	0.5/0.9/1.0/0.3	0.003/0.05/0.62/1.72	0.07/0.13/0.22/0.08	5.35±0.1 (2.7±0.3)[c] / 27±4 (296±25)	

Zr-Ph(2-2)

Table 3. Continuation 2.

| #	Group	Initial weight ratio MS/PDMS-E/PEOS	ε' [-]	ε'' [-]	σ' [·10^11 S/cm]	tan δ [-]	$\frac{\sigma \pm \Delta\sigma}{\epsilon \pm \Delta\epsilon}$ [MPa/%]	Characterization
					f = 0.1/1/10/100 Hz			
23		3/3(E)/1	–	–	–	–	4.1±0.4 / 4±1	Cloudy, homogeneous, yellowish, uneven
24		2/3(E)/1	4.8/3.7/3.3/3.2	2.2/0.6/0.2/0.06	0.01/0.03/0.10/0.41	0.47/0.16/0.05/0.02	5.4±0.2 / 92±78[b]	Homogeneous, transparent, yellowish
25		1/3(E)/1	5.6/4.7/3.2/2.4	21.2/2.4/1.0/0.4	0.12/0.13/0.61/2.04	3.81/0.51/0.32/0.15	3.2±0.1 / 215±20	
26		2/3(E)/2	10.6/5.2/3.9/3.6	8.6/2.2/0.6/0.2	0.05/0.13/0.33/0.89	0.81/0.43/0.14/0.04	5.2±0.3 / 9±1	
27		1/3(E)/2	10.7/4.8/3.6/3.3	10.6/2.4/0.6/0.2	0.06/0.14/0.33/0.90	0.99/0.51/0.16/0.05	8.2±0.2 / 28±2	
28	Zr-Ph(1-3)	1/3(E)/2 ~100 μm	8.0/3.8/2.7/2.4	4.4/1.8/0.5/0.1	0.02/0.10/0.28/0.76	0.55/0.47/0.18/0.06	6.0±0.2 / 52±5	
29		1/3(E*)/2	8.0/4.8/3.5/3.1	5.3/1.7/0.6/0.2	0.03/0.10/0.33/0.94	0.66/0.35/0.16/0.05	3.3±0.1 / 19±2	
30		1/3(G)/2	11.6/5.3/4.0/3.6	13.5/2.8/0.7/0.2	0.08/0.16/0.39/1.03	1.16/0.53/0.16/0.05	8.7±0.3 / 73±6	
31		1/3(E)/3	26.1/7.8/4.7/4.0	37.0/8.1/1.6/0.4	0.21/0.46/0.92/2.19	1.42/1.03/0.33/0.10	4.4±0.02 / 3±1	
32		1/3(G)/3	16.2/6.1/4.4/4.0	27.5/4.6/0.9/0.2	0.15/0.26/0.55/1.37	1.70/0.75/0.21/0.06	6.7±0.5 / 6±1	
33		0.5/3(E)/2	12.3/6.7/4.4/3.8	13.6/3.3/1.0/0.3	0.08/0.19/0.61/1.58	1.11/0.50/0.23/0.07	3.0±0.1 (4.3±0.1)[c] / 81±55 (192±18)	
34		0.5/3(E)/3	20.2/7.0/4.4/3.8	22.0/5.7/1.2/0.3	0.12/0.32/0.72/1.80	1.09/0.82/0.27/0.07	7.7±0.4 / 10±1	
35		0.25/3(E)/3	19.8/7.0/4.5/3.8	29.3/6.1/1.3/0.3	0.16/0.35/0.75/1.86	1.48/0.88/0.28/0.09	6.0±0.1 / 61±18 b	
36		0.1/3(E)/3	11.2/5.7/4.0/3.6	13.3/3.0/0.8/0.2	0.07/0.17/0.47/1.09	1.19/0.52/0.20/0.05	2.3±0.2 / 53±5	Homogeneous, slightly opalescent, yellowish
37	Zr(OPr)₄[a]	0.76/3(E)/2	3.8/3.5/3.3/3.3	0.5/0.2/0.06/0.02	0.003/0.01/0.03/0.12	0.13/0.05/0.02/0.01	2.0±0.2 / 1±1	Cloudy, yellow, very fragile

*PDMS-E pre-blocked by 3-aminopropyltriethoxysilane;

[a]The final calculated ZrO₂ content is the same as for the film Zr-Ph(1-3)/PDMS-E/PEOS = 1/3/2 (#27);

[b]Neck spreading; c values in brackets are for fast curing.
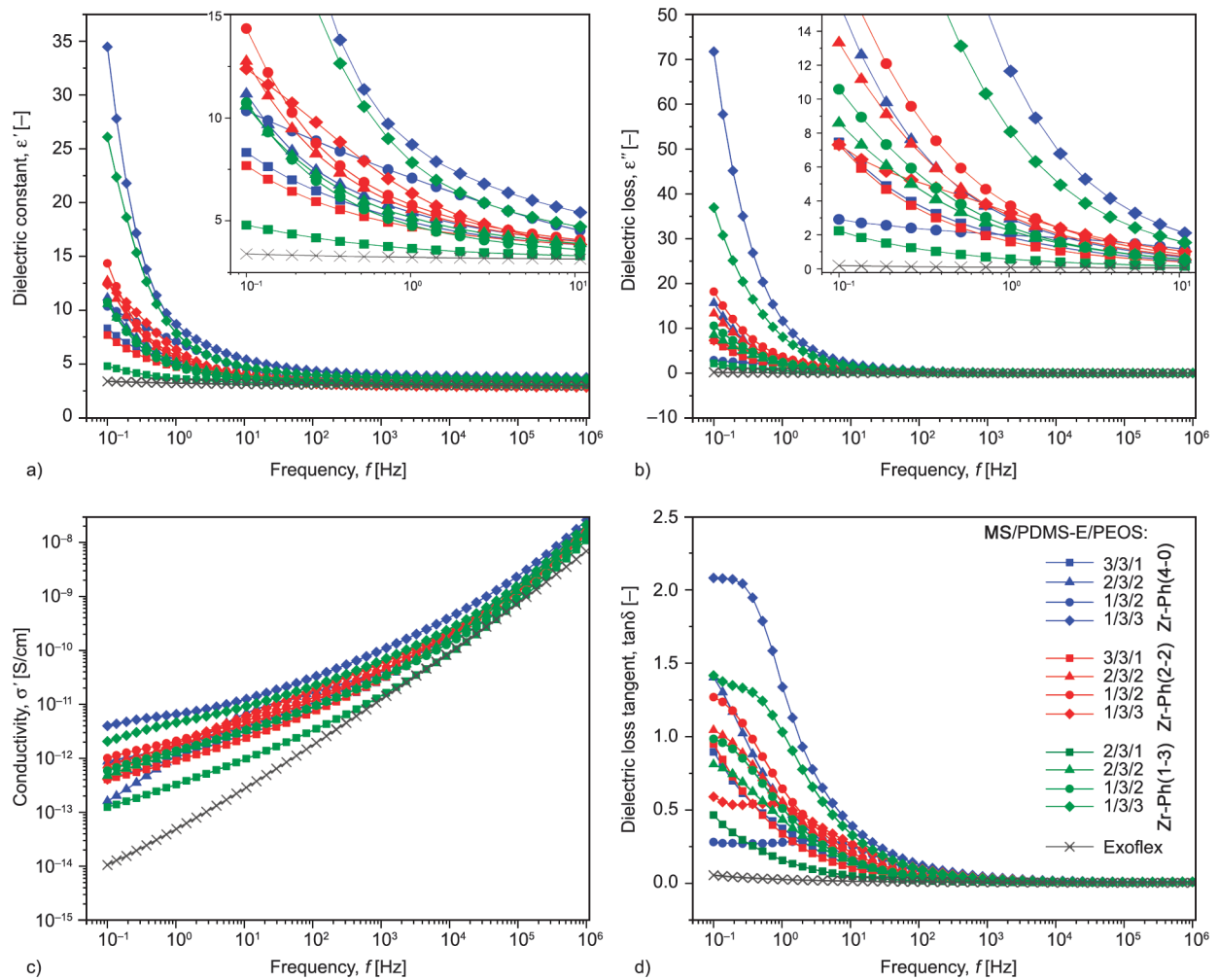
Figure 4. Frequency dependences of dielectric constant (ε') (a), dielectric loss (ε'') (b), conductivity (σ') (c), and dielectric loss tangent $\tan\delta$ (d) for three-component compositions Zr-Ph/PDMS-E/PEOS at different initial ratios.
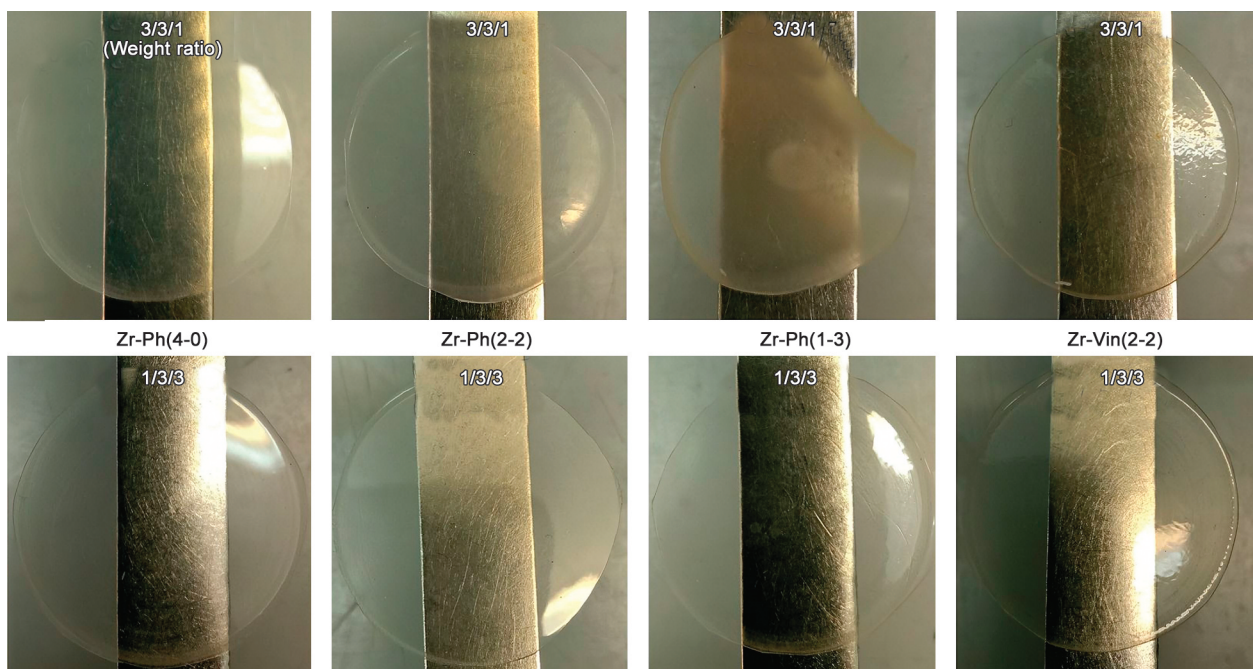
Figure 5. Photo of compositions Zr-R/PDMS-E/PEOS with various initial weight ratios.

increase in initial MS content (Figure 5). This fact may indicate either a deterioration in the compatibility of final components in the system or the formation of larger silica domains. This effect also can be explained by the presence or absence of ZrO_x units and the different content of phenyl groups in the system. In general, the dielectric constant values in the low-frequency region are higher for compositions with a maximum content of phenylsilyl substituents. At the same time, it is worth noting that the tendency of increasing ε′ with an increase in the initial PEOS/MS ratio is not always observed. So, the compositions, using Zr-Ph(2-2) as a hardener, show that this dependence is observed for the initial components MS/PDMS/PEOS ratios from 2/3/1 to 0.5/3/2 (*i.e.*, PEOS/MS = 0.5–4); however, ε′ value for the 3/3/1 ratio is higher than for 2/3/1 (Figure 6a), which can be explained by the presence of a large number of phenyl groups in the system. In the case of Zr-Ph(1-3) this dependence was investigated in more detail, expanding the number of possible ratios of the initial components (Table 3 #34–36). The high activity of such Zr-siloxane made it possible to obtain cured compositions with a minimum content of metal oxide component. It turned out that the ε′ values began to decrease again with the further increase in the PEOS/MS ratio (Figure 6b). *I.e.*, it can be concluded that the permittivity values are influenced by a combination of such factors as the functional group nature and the SiO_2 filling degree. The effect of the metal oxide component presence can be judged by the values of the dielectric parameters obtained for the reference film (Table 3 #37) cured with tetra-propoxycyrconium so that the calculated final ZrO_2 content after curing coincides with that for the Zr-Ph(1-3)/PDMS-E/PEOS = 1/3/2 composition

(Table 3 #27). It can be seen that its quality and dielectric parameters in the low-frequency region are noticeably lower than that of the cured with MS. *I.e.*, the presence of an organosilicon component in hardener also plays an important role. Film thickness reduction by ~3.5 times (Table 3 #28) leads to a certain decrease in dielectric performance in the entire frequency range.

Table 4 presents data for the compositions cured with vinyl derivatives of Zr-siloxanes. Unlike phenyl derivatives, MS structure plays a significant role here. The completely siloxy-substituted product Zr-Vin(4-0) doesn't provide films with good mechanical and electrical properties, especially with a large silica component filling (Table 4 #1). In the case of partially siloxy-substituted Zr-Vin(2-2), it is possible to obtain elastomeric compositions of good quality, as in the case of the phenyl analog Zr-Ph(2-2). The behavior of the dielectric constant values with changing the PEOS/MS ratio is the same, which indicates some general patterns of the considered compositions (Figure 6c).

Comparing materials cured using Zr-R(2-2) (where R = Me, Ph, Vin), one can trace the effect of an organic substituent at silicon atom on the films' quality and dielectric characteristics. It can be noted that the methyl substituent has practically no effect on the dielectric characteristics of films, but only the filling degree with the silica component is important. In the case of conjugate functions in the material (phenyl and vinyl) their influence on the dielectric constant values is clearly manifested; however, the main factor is still the silica filling degree. At the same time, two-component systems have similar dielectric indicators in all cases, practically coinciding with commercial silicon compounds, and with the maximum SiO_2 component
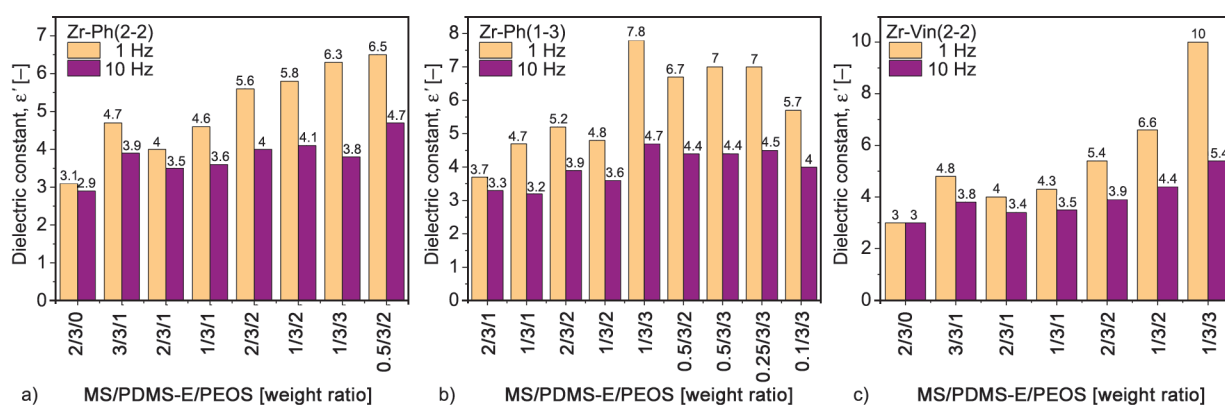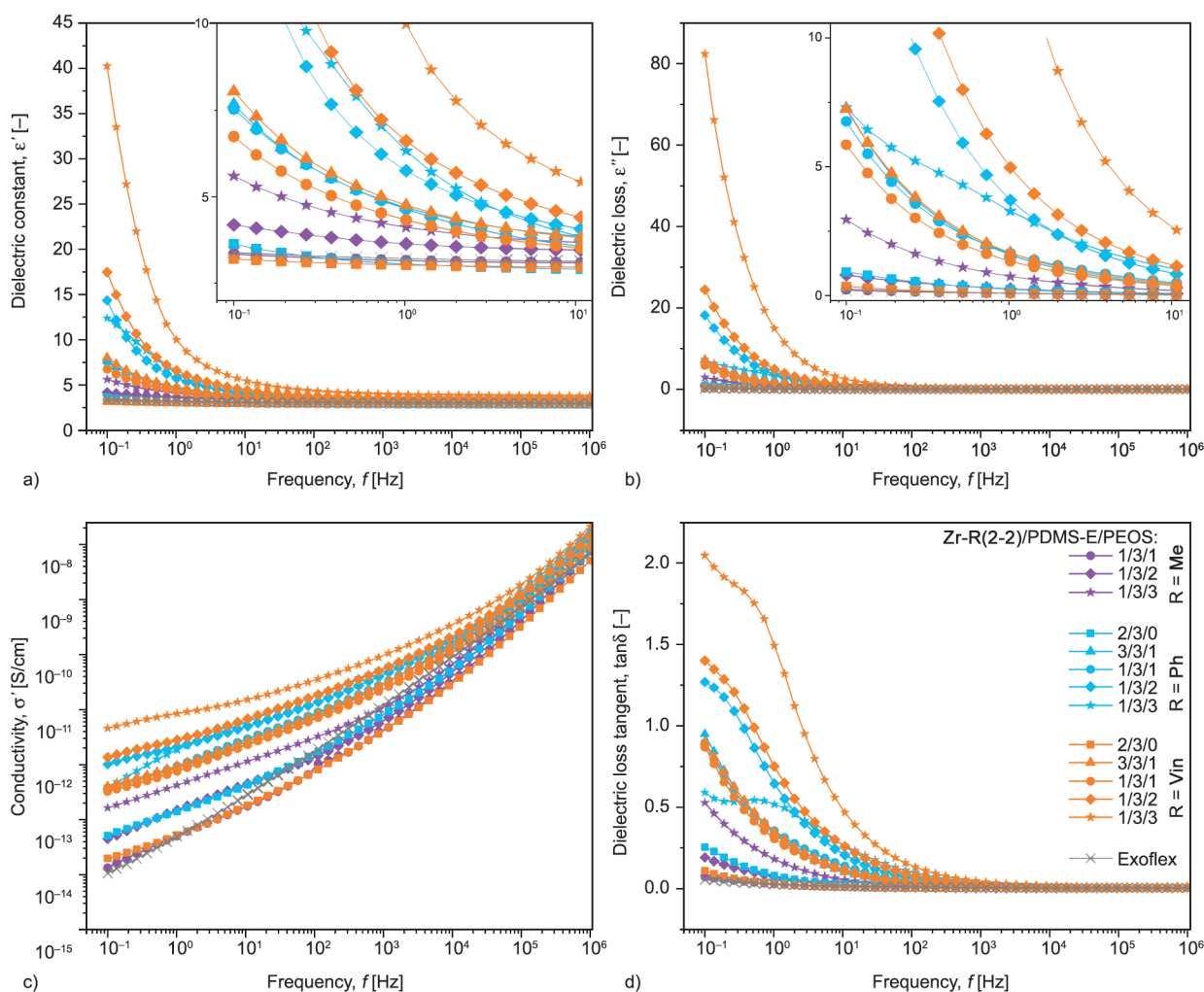

Figure 6. Dielectric constant (ε′) values dependence on the initial weight ratio Zr-R/PDMS-E/PEOS at frequencies f = 1 and 10 Hz, using Zr-Ph(2-2) (a), Zr-Ph(1-3) (b) and Zr-Vin(2-2) (c) as a hardener.

Table 4. Mechanical and dielectric characteristics at different frequencies for the compositions obtained using Zr-Vin-siloxanes.

#	Initial weight ratio MS/PDMS-E/PEOS		ε' [–]	ε'' [–]	σ' [·10^{11} S/cm]	$\tan\delta$ [–]	$\sigma \pm \Delta\sigma$ / $\varepsilon \pm \Delta\varepsilon$ [MPa/%]	Characterization
			f = 0.1/1/10/100 Hz					
1	Zr-Vin(4-0)	1/3(E)/2	2.6/2.2/2.1/2.1	0.6/0.2/0.04/0.01	0.003/0.01/0.03/0.08	0.24/0.08/0.02/0.01	–	Opalescent, curved when heated
2	Zr-Vin(2-2)	1/3(E)/0	2.8/2.8/2.7/2.7	0.2/0.04/0.02/0.01	0.001/0.003/0.01/0.05	0.05/0.02/0.01/0.003	2.2±0.2 / 455±48	Homogeneous, transparent, colorless
3		2/3(E)/0	3.2/3.0/3.0/2.9	0.4/0.1/0.03/0.01	0.002/0.005/0.02/0.08	0.11/0.03/0.01/0.01	3.6±0.4 / 646±135[a]	
4		3/3(E)/1	8.0/4.8/3.8/3.5	7.2/1.7/0.5/0.1	0.04/0.09/0.27/0.80	0.90/0.35/0.12/0.04	4.8±0.1 / 8±1	
5		2/3(E)/1	6.2/4.0/3.4/3.2	5.0/1.1/0.3/0.1	0.03/0.06/0.18/0.56	0.80/0.28/0.09/0.03	5.2±0.4 / 357±167[a]	
6		1/3(E)/1	6.7/4.3/3.5/3.3	5.9/1.3/0.4/0.1	0.03/0.08/0.23/0.67	0.87/0.31/0.11/0.04	4.6±0.3 / 271±30	Homogeneous, transparent, yellowish
7		2/3(E)/2	13.0/5.4/3.9/3.6	12.5/3.0/0.7/0.2	0.07/0.17/0.40/1.08	0.96/0.56/0.17/0.05	5.9±0.6 / 7±1	
8		1/3(E)/2	17.5/6.6/4.4/3.8	24.5/5.0/1.1/0.3	0.14/0.28/0.68/1.78	1.40/0.75/0.26/0.08	6.0±0.1 / 33±14[a]	
9		1/3(G)/2	15.2/6.2/4.2/3.7	21.0/4.4/1.0/0.3	0.12/0.25/0.59/1.52	1.38/0.70/0.23/0.07	6.3±0.1 / 165±36	
10		1/3(E)/3	40.3/10.0/5.4/4.3	82.4/14.9/2.5/0.6	0.46/0.85/1.52/3.45	2.05/1.49/0.47/0.14	7.6±0.7 / 9±1	
11		1/3(G)/3	24.8/8.3/5.1/4.2	59.5/9.4/1.9/0.5	0.33/0.53/1.12/2.57	2.40/1.12/0.37/0.09	6.8±0.1 / 76±7	
12		1/3(G)/5	63.8/14.7/6.8/5.1	132.9/25.4/4.1/1.0	0.74/1.44/2.46/5.70	2.09/1.73/0.60/0.20	6.2±0.6 / 5±1[a]	

[a]Neck spreading

Figure 7. Frequency dependences of dielectric constant (ε') (a), dielectric loss (ε″) (b), conductivity (σ') (c), and dielectric loss tangent tan δ (d) for three-component compositions Zr-R(2-2)/PDMS-E/PEOS at different initial ratios.

filling, the ε' values are maximal in the presence of vinyl substituents at the silicon atom (Figure 7).

To identify the influence of rubber type on the properties of the material, we used high-filled compositions with the initial content of Zr-R/PDMS/PEOS = 1/3/2÷1/3/5 using rubber PDMS-E* (pre-blocked with 3-aminopropyltriethoxysilane) and PDMS-G (having a molecular weight half that of PDMS-E – M_w ~ 55 000 g/mol). In 1st case, we obtain SiOEt-functional rubber and thereby regulate the rate of condensation processes in the system. In the 2nd case, we introduce ~2 times more SiOH functions, which can affect the size of the forming metal oxide and silica clusters and, as a consequence, can also affect the material elasticity. However, there are no significant changes in dielectric parameters in the frequency range $f < 10^2$ Hz when obtaining a material based on PDMS-E* (Table 3 #6, 29). But when using PDMS-G, the electrical indicators values decrease by ~10–20% in the range $f < 10^2$ Hz (Tables 3, 4). Apparently,

this is due to a decrease in the silica domains size [41]. Thus, it can be concluded that rubber also affects the dielectric characteristics of the material (Figure 8). However, its main influence are the mechanical properties of the material.

According to the measured dielectric properties of the films, the resulting materials are typical dielectrics. The dielectric constant at frequencies $f >$ 10^3 Hz weakly depends on the material composition (Figures 4a, 7a), and its value varies from 3 to 4. These values are determined by the presence of small polar groups in the material in this frequency range, in this case, residual silanol groups and groups at the silicon atom. The concentration of such groups, apparently, is small and is practically independent of the composition, so the high-frequency permittivity remains constant. The dielectric behavior of materials is also confirmed by the frequency dependence of the conductivity σ' (Figures 4c, 7c). At low frequencies σ' does not reach the plateau, *i.e.*, there is no
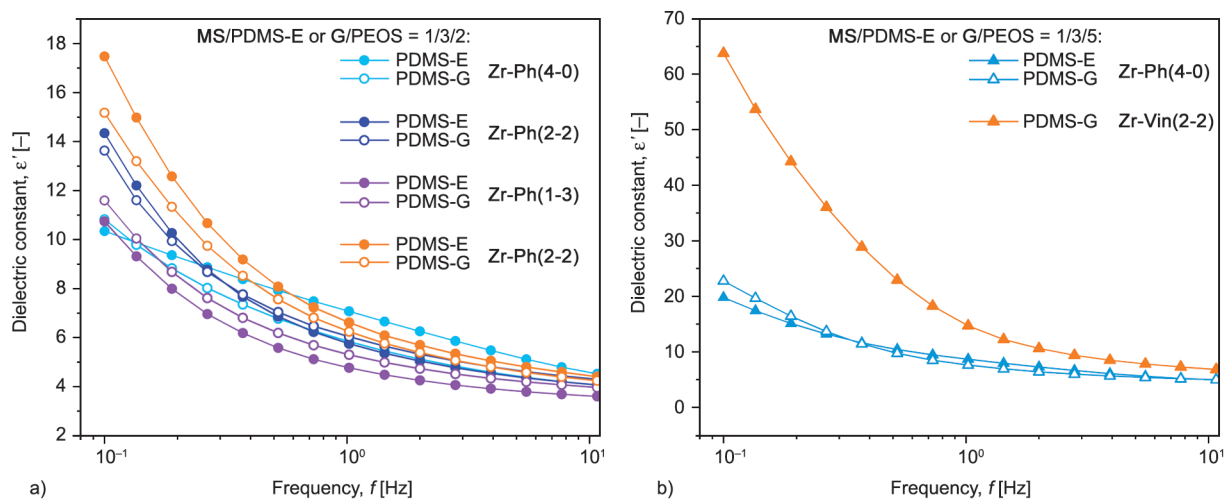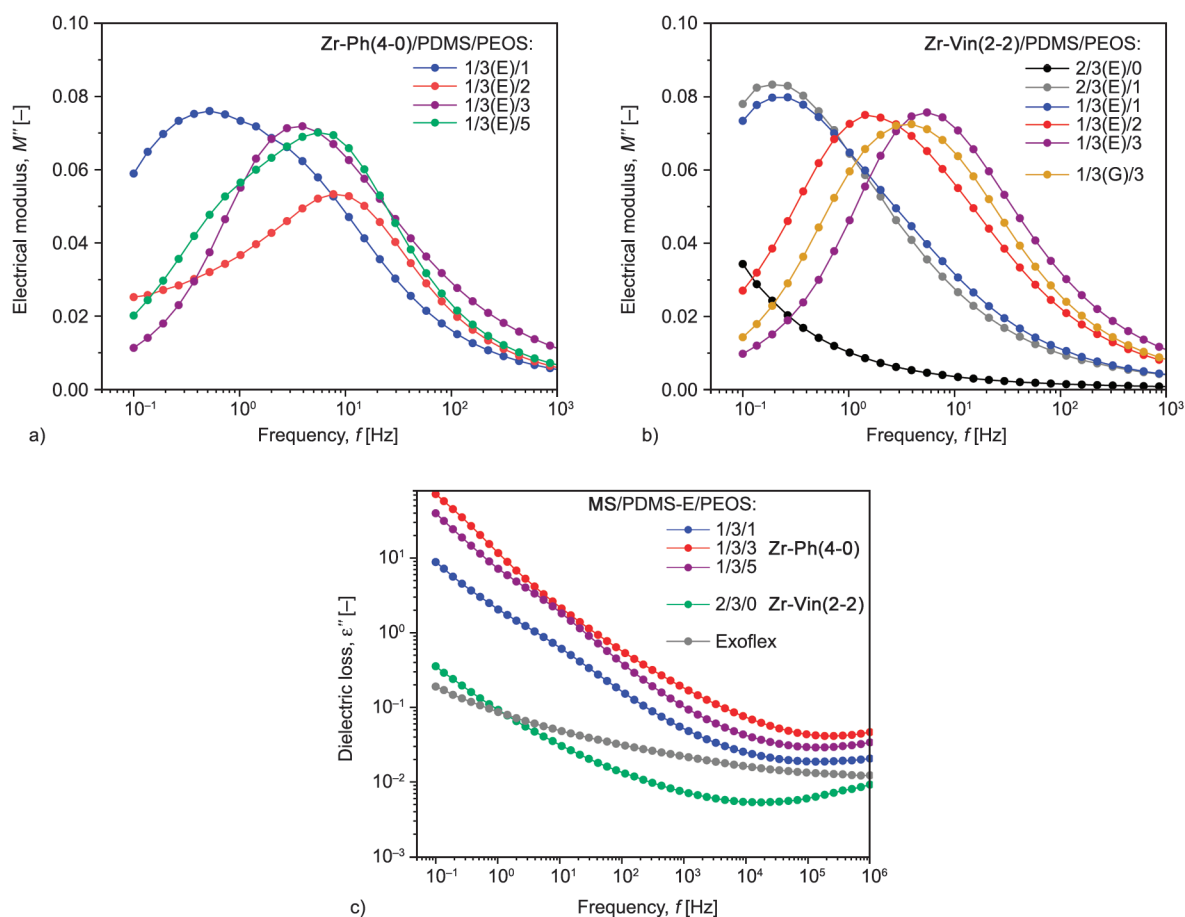
Figure 8. Frequency dependences of dielectric constant (ε') for three-component compositions Zr-R/PDMS-E or D/PEOS = 1/3/2 (a) and 1/3/5 (b) weight ratios.

bulk conductivity d_c [42]. The slope of the '$\sigma' -$ frequency' dependence equals to 1, which also indicates the absence of d_c conductivity. In the absence of the SiO$_2$ component, the dielectric constant is practically independent of the frequency (Figure 7a).

Fully different behavior is characteristic of materials in which SiO$_2$ component is formed during the curing process (Figure 1). A sharp increase in dielectric constant is observed at frequencies $f < 10^2$ Hz. At the same time, there is still no bulk dc conductivity, although the conductivity increases. The dielectric loss also increases (Figures 4b, 4d and 7b, 7d), and maxima appear on the 'imaginary module $M -$ frequency' dependencies, shifting towards high frequencies with an increase in the SiO$_2$ content (Figure 9a, 9b). At the same time, both real ε' and imaginary ε'' parts of the dielectric constant exhibit approximately linear behavior in log-log coordinates with the same slope ~0.6. In the absence of bulk conduction, and also taking into account that the conductivity does not affect the dielectric constant, this means that the dominant process at low frequencies in these systems is the charge carriers transfer in some limited, isolated regions [43, 44]. Similar behavior was observed in polymer composites based on silicone rubber [45] and epoxy resin [46, 47] containing nanoscale silica. This behavior is described by the so-called 'quasi-DC' (QDC) model [43], when there are dipoles in the system in which charges are weakly connected to each other so that they can separate and move as quasi-free ions at low frequencies. Such a case is only observed when movement is possible in limited areas without the possibility of charges becoming completely independent, as in the presence of bulk

conduction. The charges don't separate and behave like dipoles at high frequencies, which manifests itself in a weak dispersion of the permittivity, and they can separate and move mainly within the cluster at low frequencies. The QDC model has a characteristic frequency (ω_c) defining the crossover between high- and low-frequency regimes. Its presence is manifested in the appearance of a maximum on the frequency dependencies of the module M'', with its position corresponding to the beginning of ε' increase (in logarithmic coordinates). The position of M'' maximum shifts towards high frequencies with an increasing proportion of polyethoxysiloxane in initial composition. Thus, it can be assumed that the areas responsible for the low–frequency behavior of materials are SiO$_2$ component formed during the film curing, and the corresponding dipoles are, apparently, weakly bound surface silanol groups, which are also present in the formed metallosiloxane mesh. The shift of M'' maximum towards high frequencies with increasing initial polyethoxysiloxane proportion means a decrease in the size of the clusters with increasing precursor concentration. At the same time, the slope of the 'dielectric loss–frequency' dependence equal to 0.6 (Figure 9c) means that the network clusters are partially interconnected, *i.e.*, partial charge transfer between neighboring clusters is possible. A slope equal to 1 is characteristic of bulk conduction (charge movement is possible throughout the volume), and a slope equal to 0 means completely independent clusters [48]. There is an intermediate variant in our case. The charges move mainly within the clusters, moving to the boundaries during the half-period of the electric field since the slope value is >0.5, so each

Figure 9. Frequency dependences of the imaginary part of the electrical modulus M'' (a, b) and dielectric loss (ε'') (c) of films with different initial PEOS content relative to MS Zr-Ph(4-0) and Zr-Vin(2-2).

cluster acts as a very large dipole at low frequencies. And since all clusters are combined into a single network (Figure 10), the effect of an external constant electric field can cause significant cluster nodes displacements and, as a result, deformation of the material sample. It is also known that the presence of surface charge in silicone nanoscale silica leads to an increase in the dielectric response of the material [49].

The mechanical characteristics of the films were evaluated in terms of their tensile strength. Tables 2–4 present the data on the maximum stress ($\sigma \pm \Delta\sigma$) and elongation ($\varepsilon \pm \Delta\varepsilon$) at break. In general, compositions that do not contain SiO_2 are the most elastic. The presence of a silica phase in the system contributes to the material hardening and decrease in its elasticity; however, the presence of SiO_2 contributes to giving greater material tensile strength due to the effect of nanofilling. The hardening is also facilitated by an increase in the content of metallosiloxane component in the system (3/3/1 wt.pt. systems); however, at the same time, the material is capable of

developing large deformations (up to 700%) under tension, expressed in the neck formation and propagation (Figure 11a). The elasticity modulus (E) increases in the presence of a greater proportion of MS or silica component, and the effect is stronger in the case of non-fully siloxy-substituted MSs, which is associated with a stronger material hardening. But the proportion of elastic deformations, in this case, is extremely small. High SiO_2 component filling can also lead to the neck spreading during the stretching in the Zr-Ph(4-0) case (Table 3 #8, 11), which is not observed in the case of using partially siloxy substituted MS. The trend is that the use of partially siloxy-substituted MS leads to the production of stronger and less elastic compositions with the same SiO_2 filling, which may be due to greater MS activity regarding the formation of ZrOx units in the system.

The organic substituent also influences the mechanical properties of the films. When comparing the properties of films obtained using Zr-R(2-2), it can be seen that vinyl-containing compositions have a greater elasticity.
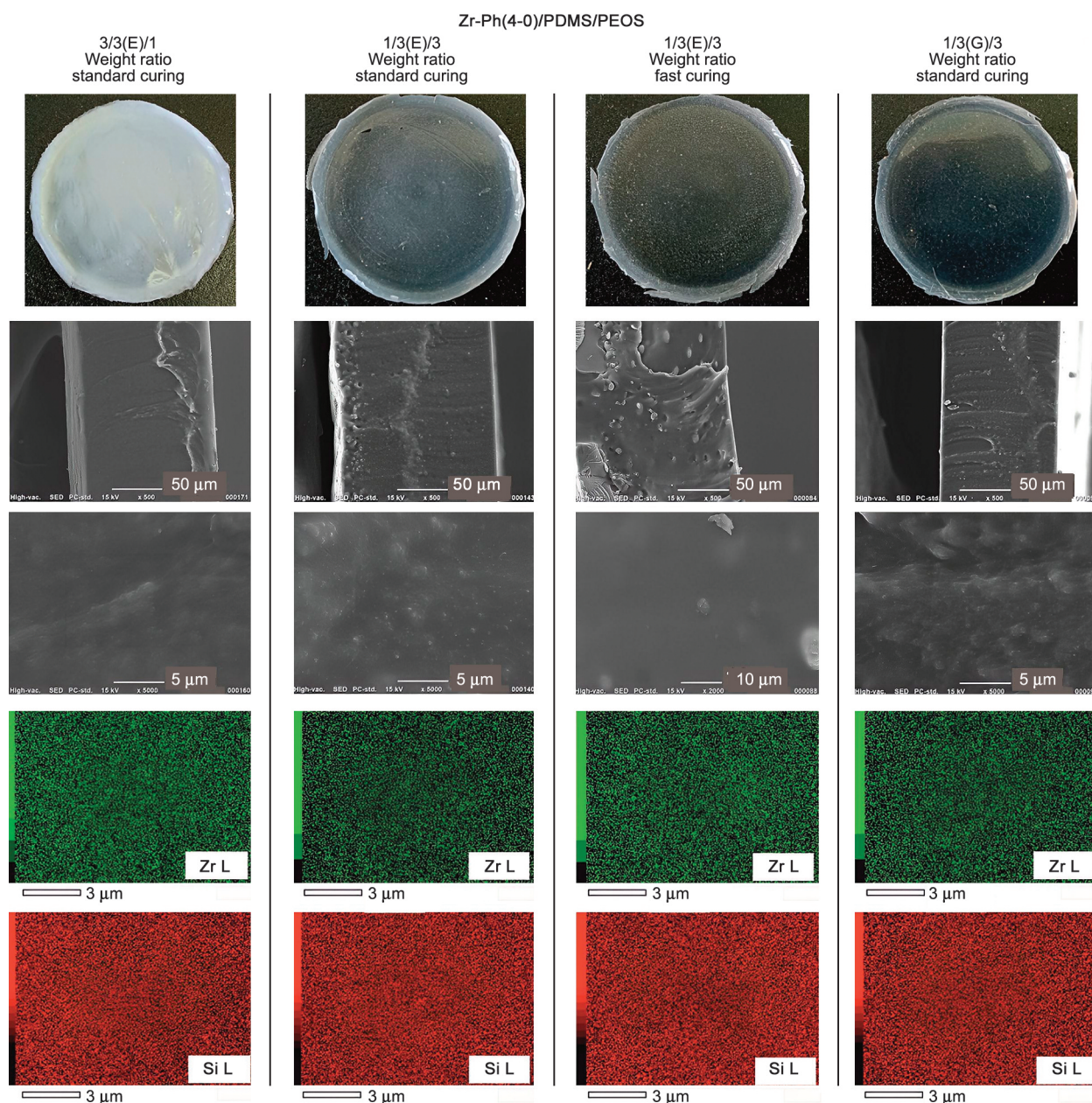
Figure 10. SEM images and element maps (Zr, Si) of ~100 μm three-component compositions Zr-Ph(2-2)/PDMS-E(G)/PEOS with various initial components content.

It turned out that the method of curing of compositions also affects the mechanical properties of the material. By concentrating the initial components solution by ~2 times (~30 wt% solution) and thereby increasing the air-drying rate of composition and reducing the air moisture access, the compositions with noticeably increased elasticity can be obtained by subsequent heating (Table 3 #5, 22, 33). However, the strength of the composition is also noticeably reduced (Figure 11b). This effect can be explained by an increase in the proportion of the organic rubber net formation due to the processes of heterofunctional condensation of silanol SiOH groups of rubber with ethoxysilyl SiOEt groups of MS and PEOS, proceeding without the additional moisture presence and slowing down the formation of an inorganic net due to faster air-drying of the mixture. *I.e.*, we get a more 'flexible' network. A similar effect is observed when using PDMS-G rubber (Table 3 #8, 9 and Table 4 #10, 11). In this case, a larger number of SiOH groups appears in the system, reacting with the functional groups of MS and PEOS, *i.e.*, we get a more developed organic network, and the elasticity of the compositions increases (Figure 11c). The effect is also expressed in a decrease in the elastic modulus of the material, presumably due to the formation of
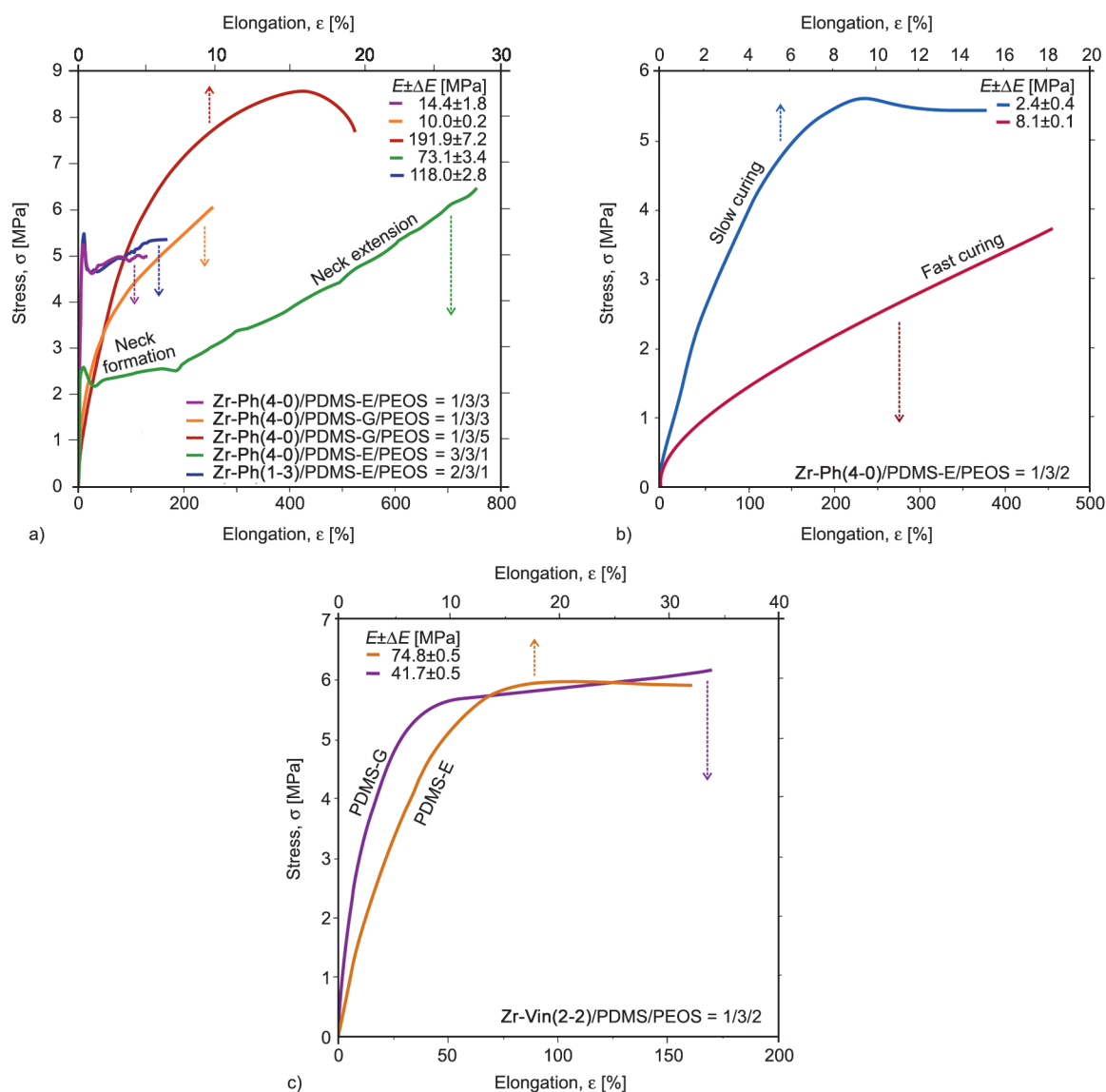
Figure 11. The stretching curves of some three-component systems: a) with the neck extension, b) at different curing rates, and c) when using rubbers of different molecular weights (*E* – Young's modulus).

smaller domains of a three-dimensional inorganic network.

SEM data (Figure 10) also confirm differences in the material morphology depending on PEOS/MS ratio, curing intensity, and rubber, which in turn affects the mechanical properties. Standard (slow) curing results in a more homogeneous material. At the same time, the use of PDMS-E rubber with a high initial PEOS content relative to MS leads to the formation of certain domains, presumably SiO_2, which occurs to a lesser extent in the case of PDMS-G rubber.

Thus, it is possible to vary the tensile strength values in the range of 5–10 MPa with an elongation at break of 10–700%, depending on the MS and rubber used, silica component filling degree, and film's curing method.

In view of the results on dielectric and mechanical properties, it can be concluded that the most promising compositions for special applications (actuators or flexible capacitive sensors) are obtained using Zr-Ph(4-0) and Zr-Vin(2-2) with lower molecular weight rubber PDMS-G and filled with a silica component in the PEOS/MS range from 3/0.5 to 3/1 (Table 3 #7, 9, 12; Table 4 #6, 9, 11).

3.2. The effect of the metal atom in hardener on the properties of compositions

Some MSs were synthesized from other metal chlorides to study the metal atom type effect. According to the data analysis obtained from using Zr-siloxanes, a number of fully siloxy substituted phenyl derivatives of Fe-, Al-, Cu-, Zn-, and W-siloxanes were
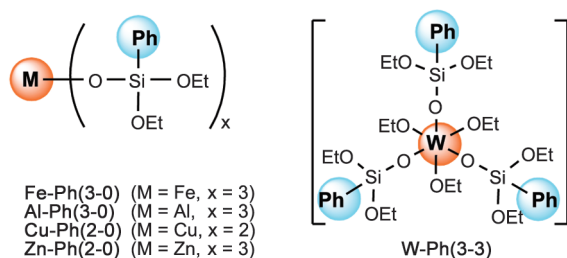
Figure 12. Phenyl derivatives of metallosiloxanes used in the work containing various metal atoms.

obtained for this study (Figure 12). MS synthesis was also carried out according to the scheme in Figure 1. Unlike Fe-Ph(3-0) and Al-Ph(3-0) obtained in a toluene medium, Cu-Ph(2-0) and Zn-Ph(2-0) metallosiloxanes were obtained in a toluene/ethanol mixture since the substitution of chlorine atoms in the corresponding chlorides requires the presence of a polar medium. In addition, despite the presence of phenyl substituent in the final product, these MSs were poorly soluble in pure toluene, so the product yield here is determined by the toluene/ethanol ratio in the mixture. Due to the great steric difficulties, it was not possible to obtain a full siloxy substituted phenyl derivative of W-siloxane W-Ph(6-0) even in a polar medium, but it was possible to obtain its partial siloxy substituted version W-Ph(3-3), containing on average equally siloxy and ethoxy substituents at the metal atom.

To study the dielectric properties, a number of two- and three-component compositions based on PDMS-E with varying the initial ratio of PEOS/MS were synthesized regarding the content of rubber similar to Zr-siloxanes (Table 5).

As can be seen from the data, the metal atom type primarily affects the kinetics of the formation of the organic and inorganic network, which is expressed in different material quality when using silanol and ethoxysilyl functional rubbers. Thus, Fe-Ph(3-0) and Al-Ph(3-0) show less activity with respect to condensation processes compared to Zr-siloxanes, which is clearly manifested with high SiO$_2$ component filling: in the 1st case, the effect of plasticity is observed expressed in small values of tensile strength with low elasticity, in the 2nd poor compatibility of the forming material components is observed, but not limited to the case of ethoxysilyl rubber (Figure 13). The use of other metallosiloxanes makes it possible to obtain a homogeneous material only when using rubber pre-blocked with 3-aminopropyltriethoxysilane, and in the case of W-Ph(3-3), such a result is

Table 5. Mechanical and dielectric characteristics at different frequencies for the compositions obtained using phenylsilyl derivatives of different metalloalkoxysiloxanes.

| #		Initial weight ratio MS/PDMS-E/PEOS	ε' [-]	ε'' [-]	σ' [·10^{11} S/cm]	tan δ [-]	σ±Δσ / ε±Δε [MPa/%]	Characterization
					f = 0.1/1/10/100 Hz			
1	Fe-Ph(3-0)	1/3/1	4.9/3.7/3.3/3.2	2.8/0.7/0.2/0.1	0.02/0.04/0.10/0.30	0.57/0.20/0.05/0.02	0.9±0.1 / 69±4	Homogeneous, transparent, brown, plasticization-like
2		1/3/2	10.4/5.9/4.3/3.9	28.9/4.3/0.9/0.2	0.16/0.24/0.52/1.26	10.39/5.87/4.31/3.89	1.7±0.1 / 21±2	
3	Al-Ph(3-0)	1/3/0	–	–	–	–	–	Cloudy, cracked
4		1/3/1	3.1/2.9/2.9/2.8	0.2/0.1/0.03/0.01	0.001/0.01/0.02/0.07	0.07/0.03/0.01/0.01	3.9±0.1 / 79±8	Cloudy, whitish
5		1/3/2	–	–	–	–	–	Cloudy, fragile, cracked
6		1/3*/2	4.2/3.5/3.3/3.2	1.0/0.3/0.1/0.03	0.006/0.02/0.05/0.16	0.24/0.09/0.03/0.01	5.0±0.4 / 174±20	Homogeneous, transparent, yellow

Table 5. Continuation.

#	Initial weight ratio MS/PDMS-E/PEOS		ε' [–]	ε'' [–]	σ' [$\cdot10^{11}$ S/cm]	tan δ [–]	$\sigma \pm \Delta\sigma$ / $\varepsilon \pm \Delta\varepsilon$ [MPa/%]	Characterization
					$f = 0.1/1/10/100$ Hz			
7	1/3/1		–	–	–	–	–	White waxy mass
8	2/3*/0	Zn-Ph(2-0)	4.0/3.8/3.7/3.2	0.2/0.1/0.2/0.6	0.001/0.004/0.09/3.47	0.06/0.02/0.04/0.17	0.6±0.03 / 571±117	Homogeneous, transparent, colorless
9	1/3*/1		4.6/3.3/2.8/2.7	1.3/0.7/0.2/0.04	0.007/0.04/0.11/2.21	0.28/0.20/0.07/0.01	1.2±0.1 / 640±52	
10	2/3*/2		6.9/4.0/3.1/3.0	9.7/1.9/0.4/0.07	0.05/0.11/0.23/0.41	1.41/0.47/0.12/0.03	0.8±0.1 / 504±105[a]	
11	2/3*/3		9.1/5.0/3.3/3.1	10.6/2.6/0.7/0.1	0.06/0.15/0.40/0.67	1.16/0.51/0.20/0.04	1.1±0.1 / 460±50	Opalescent, homogeneous, colorless
12	1/3*/2		5.2/4.1/2.9/2.6	0.7/0.8/0.5/0.1	0.004/0.05/0.28/0.57	0.14/0.20/0.17/0.04	0.8±0.04 / 405±38	
13	1/3*/3		7.2/5.3/3.5/3.0	1.8/1.2/0.8/0.2	0.01/0.07/0.50/0.98	0.26/0.23/0.24/0.06	0.9±0.1 / 555±68	
14	1/3/0	Cu-Ph(2-0)	–	–	–	–	–	Rubber doesn't cross-linked, Cu-siloxane as an individual phase
15	1/3/1		–	–	–	–	–	
16	2/3*/1		3.1/2.9/2.9/2.9	0.5/0.1/0.02/0.01	0.003/0.005/0.012/0.04	0.15/0.03/0.01/0.002	3.2±0.2 / 433±13[a]	Homogeneous, transparent, brown-green
17	1/3*/1		3.5/2.8/2.7/2.6	1.1/0.3/0.08/0.02	0.006/0.02/0.05/0.12	0.32/0.11/0.03/0.01	2.5±0.4 / 341±36	
18	1/3*/2		5.8/3.7/3.0/2.8	4.9/1.2/0.3/0.1	0.03/0.07/0.19/0.52	0.84/0.32/0.11/0.03	2.4±0.3 / 246±30	
19	1/3/0	W-Ph(3-3)	–	–	–	–	–	Not hardened
20	1/3*/0		–	–	–	–	–	Homogeneous, transparent, yellowish, but with some perspiration of uncured substance
21	1/3*/1		–	–	–	–	–	
22	0.5/0.5/3*/2	W-Ph(3-3) + Zr-Ph(2-2)	9.2/7.1/5.4/4.3	1.3/1.3/1.0/0.6	0.01/0.07/0.57/3.34	0.15/0.18/0.18/0.14	2.3±0.3 / 269±30	Opalescent, homogeneous, yellowish

*PDMS-E pre-blocked with 3-aminopropyltriethoxysilane

[a]Neck spreading

Zn-Ph(2-0)   Cu-Ph(2-0)
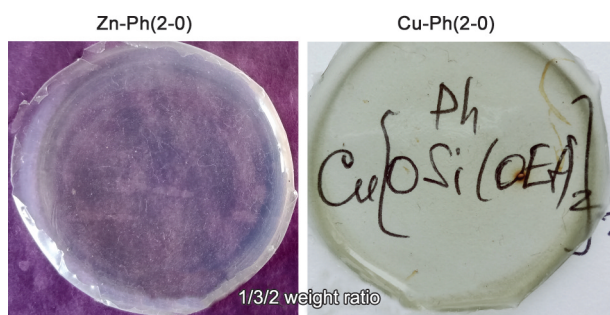
Figure 13. Photo of compositions M-Ph(2-0)/PDMS-E*/ PEOS = 1/3/2 weight ratio.

achieved only in combination with 'active' metallosiloxane, for example, Zr-Ph(2-2) (Table 5 #22). For example, a fairly rapid formation of a blue suspension was observed already at the stage of Cu-containing compositions mixing, and after warming up the residue was an inhomogeneous blue cracked mass in all cases. This fact may indicate the rapid formation of isolated from each other composition networks during the curing process. When using

pre-blocked rubber, this effect is not observed – the solution of mixed components is homogeneous, and the compositions are homogeneous and transparent after curing, although in this case, they are brown-green.

Regarding to dielectric properties, in this case, the general pattern of a sharp increase of dielectric constant in the low-frequency region $f < 10^2$ Hz with increasing silica component filling of final material is also observed. All dependencies are similar to the case of Zr-siloxanes (Figure 14). However, the influence of the metal atom on ε′ values is also traceable. Thus, it was possible to achieve the dielectric constant values, which are close to the highest ones obtained for Zr-siloxanes, only in the case of Fe-Ph(3-0), Zn-Ph(2-0) and W-Ph(3-3) (Table 5 #2, 13, 22). However, they are still lower, and the mechanical properties of the films are noticeably worse. The influence of the atom can also be traced to the nature of the dielectric constant increase. Thus, in
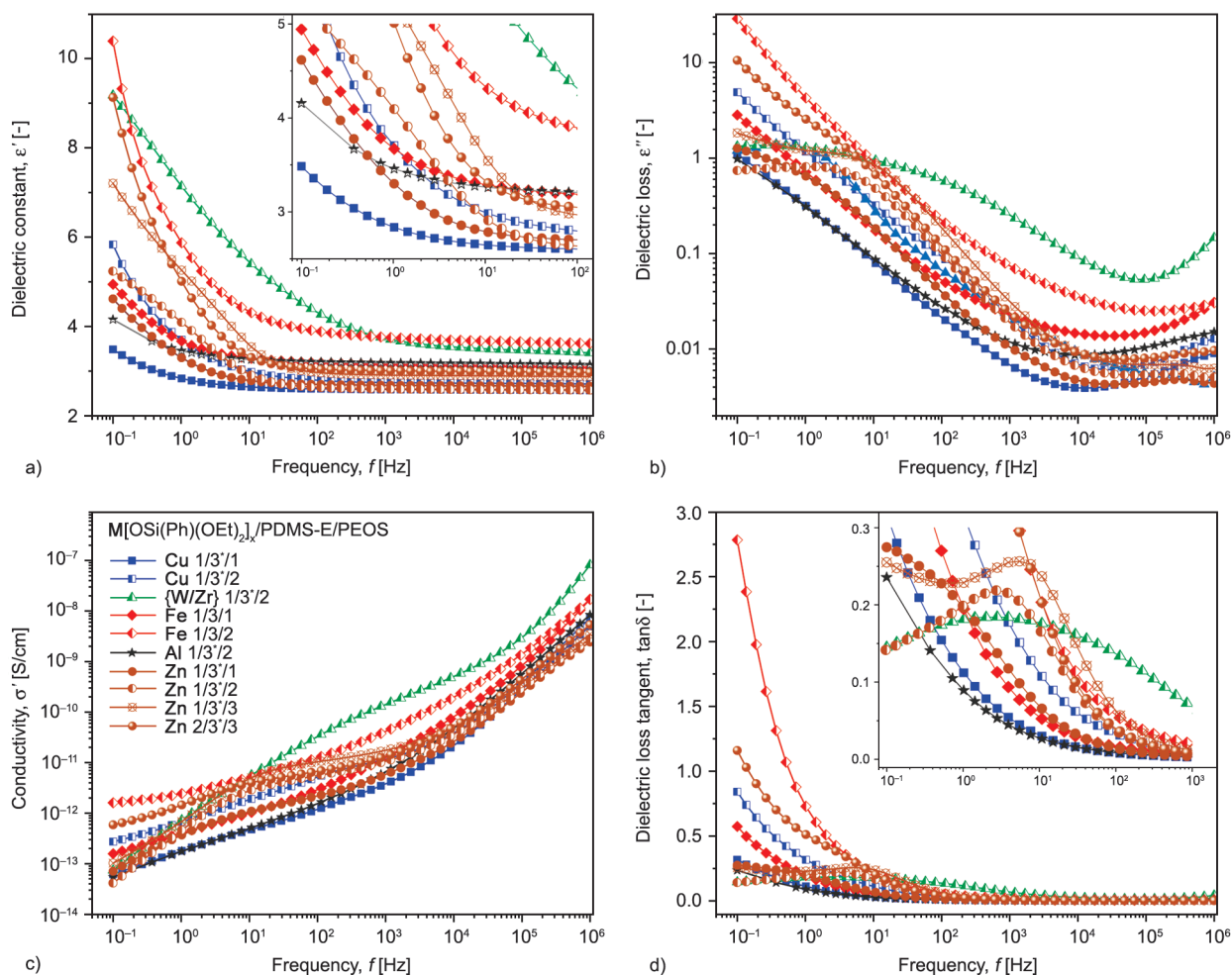
Figure 14. Frequency dependences of dielectric constant (ε′) (a), dielectric loss (ε″) (b), conductivity (σ′) (c), and dielectric loss tangent tan δ (d) for three-component compositions M[OSi(Ph)(OEt)$_2$]$_x$/PDMS-E/PEOS.
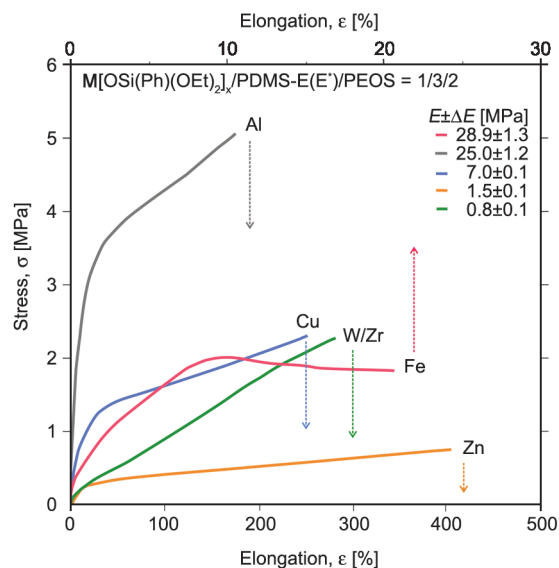
Figure 15. Stretching curves for the system $M[Si(Ph)(OEt)_2]_x$/
PDMS-E or E^*/PEOS = 1/3/2 wt.pt. (E – Young's
modulus).

the case of Fe- and W-siloxane, the ε' increase is
shifted to a higher frequency range of $f = 10^2–10^3$ Hz
compared to other MSs. And W-siloxane containing
composition characterized by the lowest dielectric
losses.

It is also possible to trace the type of metal influence
on the mechanical properties of the material. Thus,
comparing the use of Cu-Ph(2-0) and Zn-Ph(2-0), it
can be noted that the films with greater tensile
strength are obtained in the 1st case, all other condi-
tions being equal. Similar differences are observed
when comparing Al-Ph(3-0) and Fe-Ph(3-0). In gen-
eral, the use of pre-blocked ethoxysilyl-ended rubber
leads to the final material developing large deforma-
tions (Figure 15). It is obvious that the metal catalyt-
ic activity affects the rate of formation and interpen-
etration of both networks in the system and, as a
consequence, the mechanical and, in particular, the
elastic properties of the material. Among the com-
positions considered in this section, the most prom-
ising in terms of dielectric and mechanical properties
are compositions obtained using Fe-, W-, and Cu-
siloxane.

4. Conclusions

In this work, a number of highly silica component
filled compositions based on polydimethylsiloxane
were obtained, cured with various metalloal-
koxysiloxanes that differ in metal type, structure, and
organic group at the silicon atom. The dielectric and
mechanical properties of the obtained compositions

were investigated. Varying the silica filling degree
in a fairly wide range allowed us to assess the effect
of the initial components' ratio and type on the final
material properties. It is shown that the resulting sys-
tems behave like typical dielectrics. At the same
time, the introduction of a silica component in com-
bination with the formation of a metal-siloxane net-
work in the material can increase the dielectric con-
stant and conductivity compared to commercial
silicon compounds and pure PDMS in the frequency
range $f < 10^2$ Hz (ε' up to $\sim 5–10$ at 1–10 Hz). More-
over, the increase of dielectric parameters is directly
determined by the proportion of silica component in
the cured material. The nature of the frequency de-
pendences of the dielectric parameters determines
the increase of its values due to the charge carriers
transfer in some limited, isolated regions, apparently
clusters of an inorganic network. It is shown that the
variation of the organic group type at silicon atom,
metal atom type, and silica filling degree are effec-
tive tools for changing the dielectric parameters and
the increasing behavior of the dielectric constant of
the material. And by varying the rubber functionality
and length of the chain, as well as the curing rate, it
is possible to influence the strength (2–10 MPa) and
pure elastomeric properties (up to 200%) of the ma-
terial within a fairly wide range. The most promising
compositions are obtained using Zr-siloxanes
(Zr-Ph(4-0) and Zr-Vin(2-2)) with lower molecular
weight rubber PDMS-G and filled with a silica com-
ponent in the PEOS/MS range from 3/0.5 to 3/1. Be-
sides, this material formation approach allows both
the modifying of the main components and the in-
troduction of functional additives into the system
that can increase dielectric parameters and are able
to link with initial components and be evenly distrib-
uted in the final material volume. This opens up
prospects for the use of such cured systems as di-
electric elastomers for special applications such as
flexible capacitive sensors or actuators for medical
and robotic applications.

References

[1] Zhang J., Sheng J., O'Neill C. T., Walsh C. J., Wood R. J., Ryu J-H., Desai J. P., Yip M. C.: Robotic artificial muscles: Current progress and future perspectives. IEEE transactions on robotics, **35**, 761–781 (2019).
https://doi.org/10.1109/TRO.2019.2894371

[2] Brochu P., Pei Q.: Advances in dielectric elastomers for actuators and artificial muscles. Macromolecular Rapid Communications, **31**, 10–36 (2010).
https://doi.org/10.1002/marc.200900425

[3] Zhu R., Wallrabe U., Wapler M. C., Woias P., Mescheder U.: Dielectric electroactive polymer membrane actuator with ring-type electrode as driving component of a tactile actuator. Procedia Engineering, **168**, 1537–1540 (2016).
https://doi.org/10.1016/j.proeng.2016.11.455

[4] Madsen F. B., Daugaard A. E., Hvilsted S., Skov A. L.: The current state of silicone-based dielectric elastomer transducers. Macromolecular Rapid Communications, **37**, 378–413 (2016).
https://doi.org/10.1002/marc.201500576

[5] Chiba S.: Dielectric elastomers. in 'Soft actuators' (eds.: Asaka K., Okuzaki H.) Springer, Tokyo, 183–195 (2014).
https://doi.org/10.1007/978-4-431-54767-9_13

[6] Tanaka T.: Gels. Scientific American, **244**, 124–136 (1981).
https://doi.org/10.1038/scientificamerican0181-124

[7] Pelrine R., Eckerle J., Chiba S.: Review of artificial muscle approaches. in 'Third International Symposium on Micro Machine and Human Science. Nagoya, Japan' 14–16 (1992).

[8] Carpi F., Anderson I., Bauer S., Frediani G., Gallone G., Gei M., Graaf C., Jean-Mistral C., Kaal W., Kofod G., Kollosche M., Kornbluh R., Lassen B., Matysek M., Michel S., Nowak S., O'Brien B., Pei Q., Pelrine R., Rechenbach B., Rosset S., Shea H.: Standards for dielectric elastomer transducers. Smart Materials and Structures, **24**, 105025 (2015).
https://doi.org/10.1088/0964-1726/24/10/105025

[9] Kofod G., Sommer-Larsen P., Kornbluh R., Pelrine R.: Actuation response of polyacrylate dielectric elastomers. Journal of Intelligent Material Systems and Structures, **14**, 787–793 (2003).
https://doi.org/10.1177/104538903039260

[10] Lin S. Q. S., Nakos S. T.: Dual curing silicone, method of preparing same and dielectric soft-gel compositions thereof. EP0182941A1, Germany (1984).

[11] Zhenyi M., Scheinbeim J. I., Lee J. W., Newman B. A.: High field electrostrictive response of polymers. Journal of Polymer Science, **32**, 2721–2731 (1994).
https://doi.org/10.1002/polb.1994.090321618

[12] Tuichai W., Karaphun A., Ruttanapun C.: Improved dielectric properties of PVDF polymer composites filled with Ag nanomaterial deposited reduced graphene oxide (rGO) hybrid particles. Materials Research Bulletin, **145**, 111552 (2022).
https://doi.org/10.1016/j.materresbull.2021.111552

[13] McCoul D., Rosset S., Schlatter S., Shea H.: Inkjet 3D printing of UV and thermal cure silicone elastomers for dielectric elastomer actuators. Smart Materials and Structures, **26**, 125022 (2017).
https://doi.org/10.1088/1361-665X/aa9695

[14] Liu L. W., Fan J. M., Zhang Z., Shi L., Liu Y. J., Leng J. S.: Analysis of the novel strain responsive actuators of silicone dielectric elastomer. Advanced Materials Research, **47**, 298–301 (2008).
https://doi.org/10.4028/www.scientific.net/AMR.47-50.298

[15] Yu L., Madsen F. B., Hvilsted S., Skov A. L.: Dielectric elastomers, with very high dielectric permittivity, based on silicone and ionic interpenetrating networks. RSC Advances, **5**, 49739–49747 (2015).
https://doi.org/10.1039/C5RA07375H

[16] Hemeda O. M., Henaish A. M. A., Salem B. I., El-Sbakhy F. S., Hamad M. A.: The dielectric and magnetic properties of RTV-silicon rubber Ni–Cr ferrite composites. Applied Physics A, **126**, 121 (2020).
https://doi.org/10.1007/s00339-020-3297-y

[17] Babu S., Singh K., Govindan A.: Dielectric properties of $CaCu_3Ti_4O_{12}$–silicone resin composites. Applied Physics A, **107**, 697–700 (2012).
https://doi.org/10.1007/s00339-012-6885-7

[18] Saji J., Khare A., Choudhary R. N. P., Mahapatra S. P.: Visco-elastic and dielectric relaxation behavior of multiwalled carbon-nanotube reinforced silicon elastomer nanocomposites. Journal of Polymer Research, **21**, 341 (2014).
https://doi.org/10.1007/s10965-013-0341-z

[19] Huang J., Wang F., Ma L., Zhang Z., Meng E., Zeng C., Zhang H., Guo D.: Vinylsilane-rich silicone filled by polydimethylsiloxane encapsulated carbon black particles for dielectric elastomer actuator with enhanced out-of-plane actuations. Chemical Engineering Journal, **428**, 131354 (2022).
https://doi.org/10.1016/j.cej.2021.131354

[20] Paszkiewicz S., Taraghi I., Szymczyk A., Huczko A., Kurcz M., Przybyszewski B., Stanik R., Linares A., Ezquerra T. A., Rosłaniec Z.: Electrically and thermally conductive thin elastic polymer foils containing SiC nanofibers. Composites Science and Technology, **146**, 20–25 (2017).
https://doi.org/10.1016/j.compscitech.2017.04.016

[21] Wang X., Xia Z., Zhao C., Huang P., Zhao S., Gao M., Nie J.: Microstructured flexible capacitive sensor with high sensitivity based on carbon fiber-filled conductive silicon rubber. Sensors and Actuators A: Physical, **312**, 112147 (2020).
https://doi.org/10.1016/j.sna.2020.112147

[22] Liu H., Zhang L., Yang D., Yu Y., Yao L., Tian M.: Mechanical, dielectric, and actuated strain of silicone elastomer filled with various types of TiO_2. Soft Materials, **11**, 363–370 (2013).
https://doi.org/10.1080/1539445X.2012.661821

[23] Zha J-W., Dang Z-M., Li W-K., Zhu Y-H., Chen G.: Effect of micro-Si_3N_4-nano-A_l2O, sub > 3 *co*-filled particles on thermal conductivity, dielectric and mechanical properties of silicone rubber composites. IEEE Transactions on Dielectrics and Electrical Insulation, 21, 1989-1996 (2014).
https://doi.org/10.1109/TDEI.2014.004330

[24] Yu L., Skov A. L.: ZnO as a cheap and effective filler for high breakdown strength elastomers. RSC Advances, **7**, 45784–45791 (2017).
https://doi.org/10.1039/c7ra09479e

[25] Guo J., Wang X., Jia Z., Wang J., Chen C.: Nonlinear electrical properties and field dependency of BST and nano-ZnO-doped silicone rubber composites. Molecules, **23**, 3153 (2018).
https://doi.org/10.3390/molecules23123153

[26] Yang H., Yuan L., Yao X., Zheng Z., Fang D.: Monotonic strain sensing behavior of self-assembled carbon nanotubes/graphene silicone rubber composites under cyclic loading. Composites Science and Technology, **200**, 108474 (2020).
https://doi.org/10.1016/j.compscitech.2020.108474

[27] Kumar V., Alam M. N., Manikkavel A., Song M., Lee D-J., Park S-S.: Silicone rubber composites reinforced by carbon nanofillers and their hybrids for various applications: A review. Polymers, **13**, 2322 (2021).
https://doi.org/10.3390/polym13142322

[28] Faiza, Khattak A., Rehman A. U., Ali A., Mahmood A., Imran K., Ulasyar A., Zad H. S., Ullah N., Khan A.: Multi-stressed nano and micro-silica/silicone rubber composites with improved dielectric and high-voltage insulation properties. Polymers, **13**, 1400 (2021).
https://doi.org/10.3390/polym13091400

[29] Kopylov V. M., Kostyleva E. I., Kostylev I. M., Koviazin A. V.: Silica fillers for silicone rubber. International polymer science and technology, **38**, 35–47 (2011).
https://doi.org/10.1177/0307174X1103800408

[30] Dong X., Niu C., Qi M.: Enhancement of electrorheological performance of electrorheological elastomers by improving TiO_2 particles/silicon rubber interface. Journal of Materials Chemistry C, **4**, 6806–6815 (2016).
https://doi.org/10.1039/C6TC01447J

[31] Perju E., Cuervo-Reyes E., Shova S., Opris D. M.: Synthesis of novel cyclosiloxane monomers containing push–pull moieties and their anionic ring opening polymerization. RSC Advances, **8**, 7569–7578 (2018).
https://doi.org/10.1039/c8ra00707a

[32] Liao Y., Weng Y., Wang J., Zhou H., Lin J., He S.: Silicone rubber composites with high breakdown strength and low dielectric loss based on polydopamine coated mica. Polymers, **11**, 2030 (2019).
https://doi.org/10.3390/polym11122030

[33] Dascalu M., Dünki S. J., Quinsaat J-E. Q., Ko Y. S., Opris D. M.: Synthesis of silicone elastomers containing trifluoropropyl groups and their use in dielectric elastomer transducers. RSC Advances, **5**, 104516–104523 (2015).
https://doi.org/10.1039/c5ra16132k

[34] Sheima Y., Caspari P., Opris D. M.: Artificial muscles: Dielectric elastomers responsive to low voltages. Macromolecular Rapid Communications, **40**, 1900205 (2019).
https://doi.org/10.1002/marc.201900205

[35] Sheima Y., Yuts Y., Frauenrath H., Opris D. M.: Polysiloxanes modified with different types and contents of polar groups: Synthesis, structure, and thermal and dielectric properties. Macromolecules, **54**, 5737–5749 (2021).
https://doi.org/10.1021/acs.macromol.1c00362

[36] Huang T., Yuan B., Tang J., Zhang Y.: Enhanced electromechanical performance through chemistry graft copper phthalocyanine to siloxane-modified polyurethane and interpenetrate with siloxane silicon rubber as composite actuator material. IET Nanodielectrics, **4**, 38–44 (2021).
https://doi.org/10.1049/nde2.12008

[37] Tarasenkov A. N., Tebeneva N. A., Parshina M. S., Meshkov I. B., Vasilenko N. G., Cherkaev G. V., Goncharuk G. P., Katsoulis D. E., Muzafarov A. M.: New functional metallosiloxanes with partially siloxy substituted metall atom and their use in silicone compositions. Journal of Organometallic Chemistry, **906**, 121034 (2020).
https://doi.org/10.1016/j.jorganchem.2019.121034

[38] Kazakova V. V., Rebrov E. A., Myakushev V. D., Strelkova T. V., Ozerin A. N., Ozerina L. A., Chenskaya T. B., Sheiko S. S., Sharipov E. Y., Muzafarov A. M.: From a hyperbranched polyethoxysiloxane toward molecular forms of silica: A polymer-based approach to the monitoring of silica properties. ACS Symposium Series, **729**, 503–515 (2000).
https://doi.org/10.1021/bk-2000-0729.ch034

[39] Tebeneva N. A., Meshkov I. B., Tarasenkov A. N., Polshchikova N. V., Kalinina A. A., Buzin M. I., Serenko O. A., Zubavichus Y. V., Katsoulis D. E., Muzafarov A. M.: Polyfunctional branched metallosiloxane oligomers and composites based on them. Journal of Organometallic Chemistry, **868**, 112–121 (2018).
https://doi.org/10.1016/j.jorganchem.2018.04.011

[40] Andropova U., Serenko O., Tebeneva N., Tarasenkov A., Askadskii A., Afanasyev E., Novikov L., Chernik V., Voronina E., Muzafarov A.: New oligomeric metallosiloxane – polyimide nanocomposites for anti-atomic-oxygen erosion. Polymer Degradation and Stability, **183**, 109424 (2021).
https://doi.org/10.1016/j.polymdegradstab.2020.109424

[41] Zha J-W., Zhu Y-H., Li W-K., Bai J., Dang Z-M.: Low dielectric permittivity and high thermal conductivity silicone rubber composites with micro-nano-sized particles. Applied Physics Letters, **101**, 062905 (2012).
https://doi.org/10.1063/1.4745509

[42] Dyre J. C., Schrøder T. B.: Universality of AC conduction in disordered solids. Reviews of Modern Physics, **72**, 873–892 (2000).
https://doi.org/10.1103/RevModPhys.72.873

[43] Dissado L. A., Hill R. M.: Anomalous low-frequency dispersion. Near direct current conductivity in disordered low-dimensional materials. Journal of the Chemical Society, Faraday Transactions 2: Molecular and Chemical Physics, **80**, 291–319 (1984).
https://doi.org/10.1039/F29848000291

[44] Jonscher A. K.: Low-frequency dispersion in carrier-dominated dielectri. Philosophical Magazine B, **38**, 587–601 (1978).
https://doi.org/10.1080/13642817808246336

[45] Gao Y., Liang X., Dissado L. A., Dodd S. J., Chalashkanov N. M.: Dielectric response of filled high temperature vulcanized silicone rubber. IEEE Transactions on Dielectrics and Electrical Insulation, **23**, 3683–3695 (2016).
https://doi.org/10.1109/TDEI.2016.006057

[46] Yang G., Cui J., Ohki Y., Wang D., Li Y., Tao K.: Dielectric and relaxation properties of composites of epoxy resin and hyperbranched-polyester-treated nanosilica. RSC Advances, **8**, 30669–30677 (2018).
https://doi.org/10.1039/C8RA05846F

[47] Fothergill J. C., Nelson J. K., Fu M.: Dielectric properties of epoxy nanocomposites containing TiO/sub 2/, Al/sub 2/O/sub 3/ and ZnO fillers. in 'The 17th Annual Meeting of the IEEE Lasers and Electro-Optics Society (LEOS). Boulder, USA' 406–409 (2004).
https://doi.org/10.1109/CEIDP.2004.1364273

[48] Dissado L. A., Hill R. M.: The fractal nature of the cluster model dielectric response functions. Journal of Applied Physics, **66**, 2511 (1989).
https://doi.org/10.1063/1.344264

[49] Wu C., Gao Y., Liang X., Gubanski S. M., Wang Q., Bao W., Li S.: Manifestation of interactions of nanosilica in silicone rubber investigated by low-frequency dielectric spectroscopy and mechanical tests. Polymers, **11**, 717 (2019).
https://doi.org/10.3390/polym11040717